HYDROLOGICAL MODELLING OF UNGAUGED CATCHMENTS – A CASE STUDY OF THE LOWER KARIBA CATCHMENT

by

Bob Biemba Mwangala

ADissertation submitted to School of Engineering, University of Zambia in partial fulfilment of the requirement for the Master of Engineering in Water Resource Engineering

THE UNIVERSITY OF ZAMBIA
LUSAKA
2019

COPYRIGHT DECLARATION

I ***Bob Biemba Mwangala***, confirm that this work submitted for assessment is my own and is expressed in my own words. Any uses made within it of the works of other authors in any form (e.g. ideas, equations, figures, text, tables, programmes) are properly acknowledged at the point of their use. A full list of the references employed has been included.

Signed:

Date: November 2019

APPROVAL

This Dissertation of Bob Biemba Mwangala is approved as fulfilling the requirement of the Degree for the Master of Engineering in Water Resource Engineering by the University of Zambia.

Examiner 1

Name:…… Signature:…….. Date:…….

Examiner 2

Name:…….. Signature:…… Date……

Examiner 3

Name:……. Signature:…… Date……

Chairperson

Name:……. Signature:…… Date:…….

Supervisor

Name:…… Signature:…… Date:…….

ABSTRACT

In catchment hydrology, it is practically impossible to measure everything we would like to know about the hydrological system, mainly due to high catchment heterogeneity, the limitations of measurement techniques and the cost involved in collecting and processing the hydrological data, hence many catchments around the world remain poorly gauged. The Lake Kariba lower catchment is such a catchment that is not fully gauged. There is however a prospect of a less costly way of estimating lower catchment inflows using hydrological modelling techniques coupled with the use of free satellite data to simulate flows in the Lake Kariba Lower Catchment.

RS MINERVE software was used to simulate surface run-off for poorly gauged Lower Kariba Catchment. The integrated rainfall-runoff model HBV was used for calibration and validation, with the model performing satisfactory at monthly time step, with the average runoff of the lower Kariba catchments being approximately 12% of the total yearly runoff recorded at Victoria Falls gauging station. Open source Geographic Information System (GIS) Software QGIS was used to derive drainage networks from DEM for the sub basins, the outflow point of the catchments.

The model's results showed good correlation with observed data giving a Nash Sutcliffe coefficient of 0.82, Pearson correlation of 0.89 and Bias score of 0.94 for the Sanyati flows while Gwayi flows gave 0.64, 0.87 and 0.98 respectively for the same indicators after calibration. The simulation results obtained from the model can be used in many water resources management activities.

Keywords: DEM, HBV, Hydrological Model, QGIS, RS Minerve, Satellite Data, Ungauged Catchments.

DEDICATION

To my Dear Wife, Racheal and our Children:
Nalishebo, Mushiba and Mate

... You guys have made me reach this far!

ACKNOWLEDGEMENTS

First and foremost, I wish to thank my God and Creator for His mercies that are ‘new every morning.’

I am immensely grateful to the entire Academic Staff at University of Zambia for their valuable guidance in all my studies. I sincerely thank my supervisor, Dr. Edwin Nyirenda who had been quite patient with me and diligently guided the current study. His advice at all stages of this thesis have been invaluable. Special thanks also go to my employers, the Zambezi River Authority for the permission to use the data in my dissertation through the Director of Water Resources and Environmental Monitoring, Engineer Christopher Chisense and my colleagues at work for that valuable advice you gave me, not forgetting Engineer Samuel Mwale and John Bonzo for your input in this study.

Lastly, but by no means the least, I wish to thank my dear wife, Racheal and the entire Mwangala “Kingdom” for their moral support and patience during the long hours spent with books in their stead. Opinions, findings and conclusions or recommendations expressed and any errors contained in this Thesis are solely mine.

TABLE OF CONTENTS

LIST OF TABLES

LIST OF FIGURES

ABBREVIATIONS AND ACRONYMS

ARMA	Autoregressive Moving Average Model
BLUE	Best Linear Unbiased Estimator
BS	Bias Score (BS)
CPU	central processing unit
DEM	Digital Elevation Model
FAO	Food and Agriculture Organization
FSL	Full Supply Level
GIS	Geographic Information System
Giovanni	Geospatial Interactive Online Visualization And Analysis Infrastructure
GOES	The Geostationary Operational Environmental Satellite system
HBV	Hydrologiska Byråns Vattenbalansavdelning
ITCZ	Inter Tropical Convergence Zone
LWIR	Long-Wave Infrared
MWIR	Middle-Wave Infrared
NSC	Nash-Sutcliffe Coefficient
NASA	National Aeronautics and Space Administration
NIMA	National Imagery and Mapping Agency
NOAA	National Oceanic and Atmospheric Administration
Pbias	Percent Bias
RS	Remote Sensing
SWIR	Short-Wave Infrared
SCE-UA	Shuffled Complex Evolution – University of Arizona
SWAT	Soil Water Assessment Tool
SADC	Southern Africa Development Community
SRTM	Shuttle Radar Topography Mission
SAR	Synthetic Aperture Radar
TIROS-N	Television Infrared Observation Satellite
TRMM	Tropical Rainfall Measuring Mission
UAMC	Uniform Adaptative Monte Carlo
VNIR	Visible and Near Infrared
ZRA	Zambezi River Authority

CHAPTER 1: INTRODUCTION

1.1 Background

The Zambezi River is Southern Africa's largest river. It rises in the hills between Zambia and the Democratic Republic of Congo. The course of the river has the general West-East trend flowing a distance of 2,700km before discharging into the Indian Ocean in Beira port of Mozambique. The Kariba Dam that was constructed in the late 1950s primarily for hydro-electric power for mines in Northern and Southern Rhodesia (now Zambia and Zimbabwe) is located just almost at the center of the Zambezi River water course (Federal Power Board, 1959). Downstream of the Kariba Dam is the Cahora Bassa Dam in Mozambique. These dams are managed by different Institutions, for Kariba Dam, the Zambezi River Authority (ZRA) is the statutory body jointly owned by the Governments of Zambia and Zimbabwe whose mission is to effectively utilize the water and other resources of the Zambezi River common to the borders of the two countries (ZRA, 2010). The reservoir behind the Kariba Dam has a live storage capacity of nearly 65 km^3 (Southern Africa Development Community(SADC), 1994). The catchment above the Lake Kariba is divided into the Upper Catchment with an Area of 507 200km^2, whose outlet is the Victoria Falls and the Lower Catchment of 156 600km^2, which lies between the Victoria Falls and the Lake, including the areas surrounding the lake (Shawinigan Engineering, 1993).

In catchment hydrology, it is practically impossible to measure everything one would like to know about the hydrological system, mainly due to high catchment heterogeneity, the limitations of measurement techniques and the cost involved in collecting and processing the hydrological data, hence many catchment around the world remain poorly gauged (Bloschl & Sivapalan, 1995). The Lake Kariba lower catchment is such a catchment that is not fully gauged. There is however a prospect of a less cost way of estimating lower catchment flows using hydrological modelling techniques coupled with the use of satellite data. Modelling the rainfall–runoff behavior of ungauged catchments in the Lower Lake Kariba Catchment is of interest both for understanding systems behavior and as a basis of sustainable water resources management (Tan, et al., 2014). Rainfall-runoff modeling at ungauged catchments often involves the transfer of calibrated model parameters from "donor" gauged catchments to the ungauged catchments (Lenhart, et al., 2002).

This study intends to generate flows for Lake Kariba Lower catchment that will be used for water supply management, legal settlements – such as, water rights, interstate agreements and court decrees, engineering design, operations, assessing impacts – water diversions, changing land management & climate change, flood planning, management & warning systems, streamflow forecasting, water quality monitoring, and ecosystem & recreational management.

1.2 Problem Statement

The total runoff inflow in Lake Kariba can be divided into two components; the first component is runoff from the upper catchment whose outlet is at Victoria Falls, which currently represents the best estimate of inflow as this has a stable discharge rating curve (ZRA, 2005). The second part consists of inflow from the lower catchment which is poorly gauged (Shawinigan Engineering, 1993). Local inflow into the lake from the lower catchment is imperfectly known (Batoka Joint Venture, 1993) as the current estimation of the water flux coming into the Lake from the Kariba lower catchment is based on the statistical analyses of historical data, the demands of water, the existing lake water level and storage available for water banking, resulting in zero or negative flows during the dry season (Tumbare, 2000).

In view of the above challenge of estimating lower catchment inflows into Lake Kariba, there is need to fully gauge the rivers around the Lake if meaningful management of the lake and other water resources needs are to be achieved. While this option remains practically impossible given that these rivers are annual streams as they dry up just after the rainy season, coupled with the cost that is attached in coming up with new gauging stations, ZRA paying for personnel who take care of these stations including the salaries during the five to seven months (Santa, 1978) when the rivers are not contributing anything to the inflow into the lake. There is however a prospect of a less cost way of estimating lower catchment inflows using Hydrological modelling techniques coupled with the use of satellite data to estimate the flows in the Lake Kariba Lower catchment.

1.3 Aim

The aim of the research was to simulate surface run-off for poorly gauged Lower Kariba Catchment using hydrological modelling software.

1.4 Objectives

The main objective of the study is to assess the flow contribution of lower Kariba catchment into Kariba Reservoir that will in turn enhance efficient water allocation and use for sustainable water resources management of Lake Kariba Lower basin using the hydrological modelling software with the use of remote sensing.

This main objective will be addressed through the following specific objectives:

- Estimate the Kariba lower catchments flows.
- Establish the hydrological model for Lake Kariba lower catchment via the result obtained from the above.

1.5 Research questions

The following research questions below were formulated in order to achieve the research objectives:

i. Can the use of DEM and satellite data augment the scarcity of hydrological data such as stream flow?

ii. How can the accuracy of the generated stream flow data be tested and using what type of a model?

1.6 Justification

Prediction of runoff water in an ungauged catchment area is vital for various practical applications. This includes efficient use of the reservoir, the design of drainage structure and flood defenses, runoff forecasting and for catchment management tasks such as water allocation and climate impact analysis. More importantly the growing populations, contaminated supplies, and potentially changing supplies, have come under much more scrutiny in the recent years. The amount of water crossing political boundaries as is the case of Lake Kariba lower catchment were water is mostly generated from Zambia and Zimbabwe, and issues of equal and equity contributions of water are constantly being raised in the political corridors, have necessitated the undertaking of this study to determine how much water is crossing political boundaries.

Further, this research attempts therefore to establish a hydrological model of Lake Kariba lower catchments that well estimates the poorly gauged lower catchment flows using hydrological modelling techniques and satellite data. This research will further add and contribute to knowledge of other similar studies that have been conducted on Lake Kariba lower catchments.

1.7 Dissertation layout

The dissertation contains 6 chapters organized as follows:

Chapter one covers the general background of the study, problem statement, aim, justification, research objectives and research methodology. Chapter two deals with a literature review on catchment hydrology, rainfall runoff models regarding ungauged catchments, and the role of Geographic information systems (GIS), and Digital elevation models (DEM) in remote rainfall-runoff modelling. Chapter three describes the study area; the description includes location, climate condition, and drainage, in the study area. Chapter four outlines data availability and processing methods that were followed. Chapter five presents and discusses the results. Finally, chapter six concludes the research findings and proposes recommendations.

CHAPTER 2: LITERATURE REVIEW

2.1 Introduction

Amongst the great unsolved challenges that Water Resources Engineers and Hydrologist alike have is to accurately simulate or predict flows without any observational data with which to calibrate a hydrological model, i.e. an ungauged Catchment; (Bloschl, 2005;Wagener, et al., 2004). Modelling the rainfall–runoff behavior of ungauged catchments is of interest both for understanding systems behavior and as a basis of sustainable water resources management. In ungauged catchments, model parameters must be estimated from other sources of information (Vogel, 2005). An appealing way to estimate model parameters in ungauged catchments is to glean the model parameters from hydrologically similar catchments. The concept of hydrological similarity assumes that the runoff response to a given rainfall input in two different catchments will be similar if similar rainfall–runoff processes occur. These processes are not known in full detail and thus different similarity concepts have been proposed in literature. The process of transferring parameters from hydrologically similar catchments to a catchment of interest is generally referred to as regionalisation (Bloschl & Sivapalan, 1995).

2.2 Catchment Hydrology

The main components of a catchment hydrology are summarized in Figure1 (Tarboton, 1997). Rainfall reaching the ground may enter the soil by infiltration or may flow down the hillslope as surface runoff. Surface water can return to the atmosphere by evaporation. Water within the root zone may be taken up by plants and subsequently released into the atmosphere by transpiration from the plant leaves. Water within the soil may produce lateral flow downslope at shallow depth or may percolate downwards to groundwater store. Water may also be drawn upwards from the subsoil by capillary action if the topsoil becomes dry. Surface runoff and shallow lateral flow may enter streams fairly quickly after the start of a storm event. Groundwater may be released to streams more slowly and over a longer period as baseflow. A detailed description of some of the process can be found in the book of Kirby, (1978) and Chow, et al., (1988).

Precipitation is the most important process for the generation of runoff at a catchment level. Though its availability is spatial and temporal, its usually in the form of snow, hail, dew and rain. For the purpose of this study, precipitation will refer to rain.

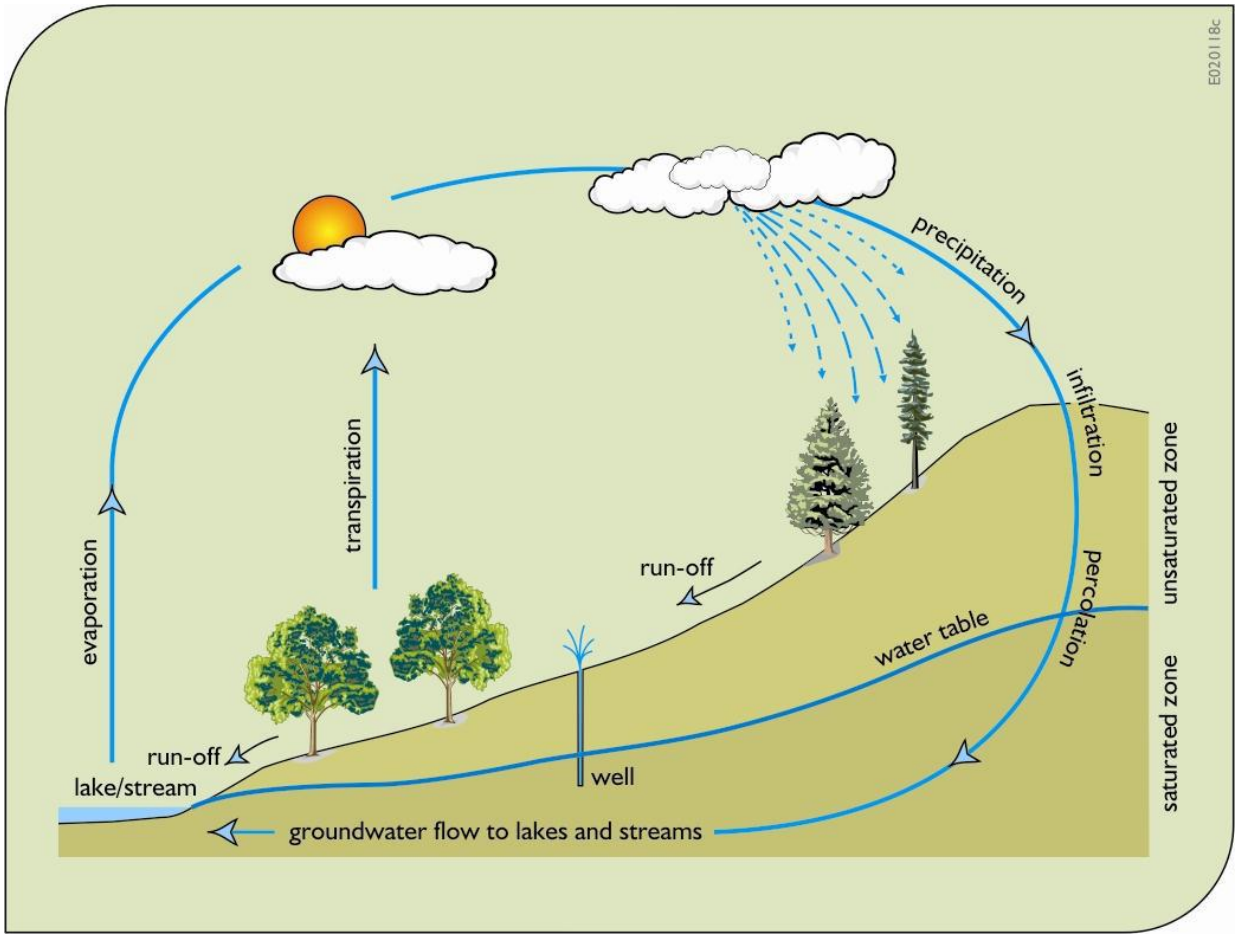

Figure 1. Physical Process Involved in Catchment Hydrology (Tarboton, 1997)

2.3 Rainfall Runoff Modelling

Sharma, et al., (2008), defined a model as a simplified representation of a real-world system. The best model is the one which give results close to reality with the use of least parameters and model complexity (Gayathri, et al., 2015). Understanding catchment hydrology is a very complex issue as most process involved are difficult to accurate quantify. Models are mainly used for predicting system behavior and understanding various hydrological processes. A model consists of various parameters that define the characteristics of the model. A runoff model can be defined as a set of equations that helps in the estimation of runoff as a function of various parameters used for describing watershed characteristics. It should be noted that a hydrological system can be generally be defined by equation 1, which is a typical hydrological system equation:

$$y = Hx \qquad \text{Equation 1}$$

where y = system output, H = system function, x = system input. The system function H determines the response, y, of the system to the system input, x. In this case y and x are called the variables of the system. The system function is often termed the model of the system

The two important inputs required for all hydrological models are rainfall data and drainage area. Along with these, water shed characteristics like soil properties, vegetation cover, watershed topography, soil moisture content, characteristics of ground water aquifer are also considered (Gayathri, et al., 2015). Hydrological models are nowadays considered as an important and necessary tool for water and environment resource management.

The alteration of rainfall to runoff process has been aided by rainfall-runoff models. These models have been under constant development for a long time now. Sing and Woolhiser (2002) have done a review of catchment models. Beven (2012) said the following in respect to availability of rainfall-runoff models over the past decade, “it is now virtually impossible for any one person to be aware of all the models that are reported in the literature”.

2.3.1 Types of Models

Rainfall-runoff models are classified based on model input and parameters and the extent of physical principles applied in the model as shown in Figure 2 below. It can be classified as lumped and distributed model based on the model parameters as a function of space and time and deterministic and stochastic models based on the other criteria. Deterministic model will give same output for a single set of input values whereas in stochastic models, different values of output can be produced for a single set of inputs. Moradkhani and Sorooshian (2008) said that in lumped models, the entire river basin is taken as a single unit where spatial variability is disregarded and hence the outputs are generated without considering the spatial processes where as a distributed model can make predictions that are distributed in space by dividing the entire catchment in to small units, usually square cells or triangulated irregular network, so that the parameters, inputs and outputs can vary spatially. Another classification is static and dynamic models based on time factor. Static model exclude time while dynamic model include time. Sorooshian et al. (2008) had classified the models as event based and continuous models. The former one produce output only for specific time periods while the latter produces a continuous output. One of the most important classifications of hydrological models is empirical model, conceptual models and physically based models. All three types of mathematical models that will be described below are useful but in somewhat different circumstances. Each has its own effectiveness, depending upon the objective of study, the degree of complexity of the problem, and the degree of accuracy desired. There is no conflict between these models; they represent different levels of approximation of reality (Xu 2002). Gayathri et al 2015, further explained the characteristics of the models as shown in Table 1 below.

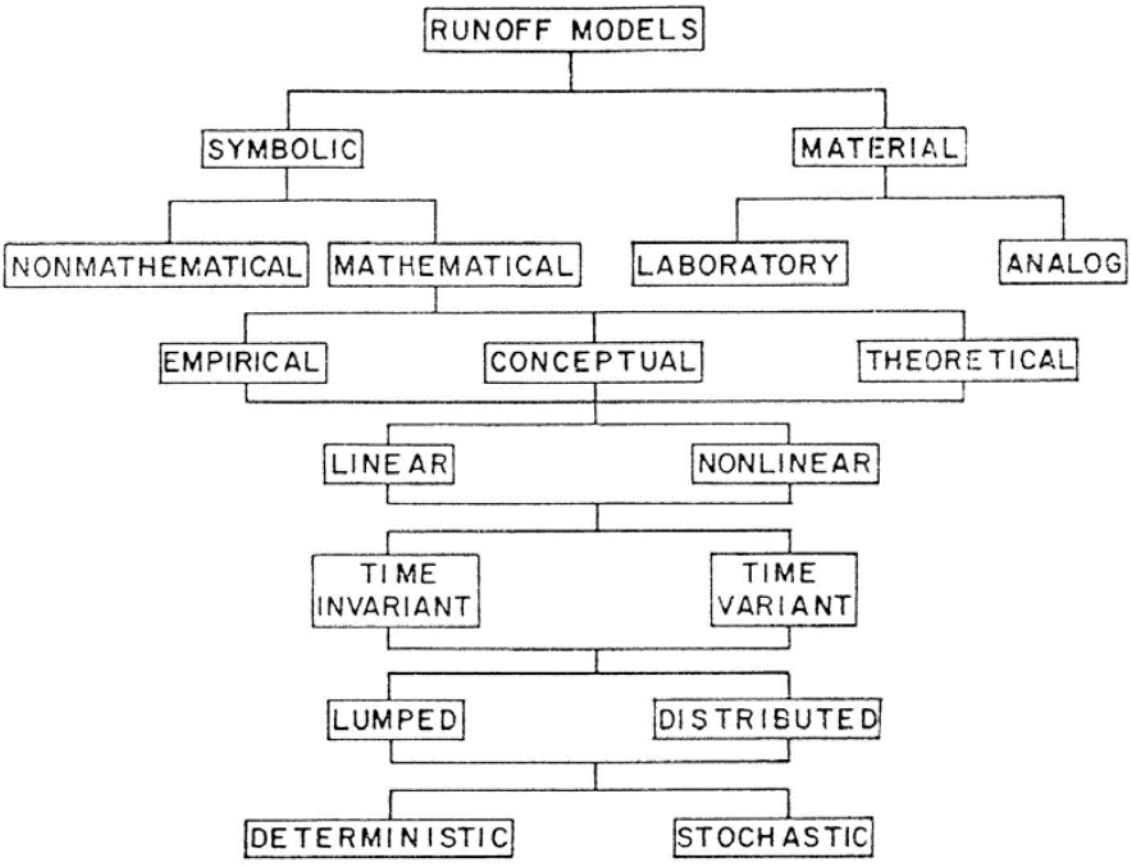

Figure 2. Classification of Hydrologic Models (Singh, 1988)

Table 1. Characteristics of Models

Empirical model	**Conceptual model**	**Physically based model**
Data based or metric or black box model	Parametric or grey box model	Mechanistic or white box model
Involve mathematical equations, derive value from available time series	Based on modeling of reservoirs and Include semi empirical equations with a physical basis.	Based on spatial distribution, Evaluation of parameters describing physical characteristics
Little consideration of features and processes of system	Parameters are derived from field data and calibration.	Require data about initial state of model and morphology of catchment

High predictive power, low explanatory depth	Simple and can be easily implemented in computer code.	Complex model. Require human expertise and computation capability.
Cannot be generated to other catchments	Require large hydrological and meteorological data	Suffer from scale related problems
ANN, unit hydrograph	HBV model, TOPMODEL	SHE or MIKESHE model, SWAT
Valid within the boundary of given domain	Calibration involves curve fitting make difficult physical interpretation	Valid for wide range of situations

Source: (Gayathri, et al., 2015)

2.3.2 Empirical Models

Empirical models (sometimes called black-box models or input output models) do not aid in physical understanding. They contain parameters that may have little direct physical significance and can be estimated only by using concurrent measurements of input and output. Examples are stochastic time series models. In many situations, empirical models can yield accurate answers and can, therefore, serve a useful tool in decision-making. The ARMA (autoregressive moving average model) is one of the examples of stochastic time series models.

2.3.3 Conceptual

Conceptual models (sometimes called grey-box models) are intermediate between theoretical and empirical models. Hydrologic models are mostly considered as conceptual, if the function establishing the relationship of the physical processes acting upon the input variable(s) to produce the output variable(s) holds for all scenarios. Generally, conceptual models consider physical laws but in highly simplified form. They are many models that belong to this class; an example which is of interest to this study is the Hydrologiska Byråns Vattenbalansavdelning (HBV) model.

2.3.4 Physically based Models

Physically based models, (sometimes called white-box models or theoretical models) presumably are the consequences of the most important laws governing the phenomena. A theoretical model has a logical structure similar to the real-world system and may be helpful under changed circumstances (Xu, 2002). Examples of theoretical models may include watershed runoff models based on St. Venant equations, infiltration models based on two phase flow theory of porous media (Morel-Seytoux, 1978), evaporation models based on theories of turbulence and diffusion (Brutsaert & Mawdsley, 1971), and groundwater models

based on fundamental transport equations (Freeze, 1971). An example of physically based models is the SHE models (Abbott, et al., 1986).

2.4 Ungauged Rainfall Runoff Modeling

Accurate and timely predictions of high and low flow events at any ungauged watershed location can provide stakeholders the information required to make strategic, informed decisions. Whenever data is not available, hydrological models are important to establish baseline characteristics and determine long term impacts which are difficult to calculate (Patil & Stieglitz, 2013). The aim of hydrological modeling in some ungauged catchments is to reduce the uncertainty in hydrological predictions. A common strategy for streamflow modeling at ungauged catchments involves the following procedure:

- calibration of model parameters at gauged catchments using the observed streamflow data, and,
- transfer of the calibrated parameters from gauged to ungauged catchments that are perceived to be hydrologically similar (Oudin, et al., 2010).

One can define two or more catchments as hydrologically similar if their daily stream responses (runoff) are highly correlated to each other (Archfield & Vogel ,2010; Patil & Stieglitz, 2012). Since streamflow data is not available at ungauged catchments, indirect characterization of hydrologic similarity becomes essential (Bloschl, 2005). Two similarity approaches, viz., spatial proximity and physical similarity, have been shown to work successfully in many regions (Patil & Stieglitz, 2013). In the spatial proximity approach, a gauged catchment that is located closest to the ungauged catchment is assumed to be hydrologically similar (Merz & Bloschl, 2004), whereas in the physical similarity approach, a gauged catchment that is most similar to the ungauged catchment in physical attribute domain is assumed to be hydrologically similar (Oudin, et al., 2010).

The concept of hydrological similarity assumes that the runoff response to a given rainfall input in two different catchments will be similar if similar rainfall–runoff processes occur These processes are not known in full detail and thus different similarity concepts have been proposed in the literature. For the Lower Kariba Catchment, it was assumed that Sanyati and Gwayi catchment are of physical similarity. The process of transferring parameters from hydrologically similar catchments to a catchment of interest is generally referred to as regionalization (Bloschl & Sivapalan, 1995). The two most widely used concepts for regionalizing model parameters are hydrological similarity as a function of spatial proximity and similarity as a function of catchment attributes. An overview of studies on regionalization of rainfall–runoff model parameters using large catchment samples is given in Table 2.

Table 2. Overview of rainfall-runoff regionalisation studies

Reference	*Country*	*Model*	*Time Step*	*Methods*
Sefton & Howarth (1998)	UK	IHACRES	Daily	Regression with catchment attributes
Peel et al. (2000	Australia	SIMHYD	Monthly	Regression with catchment attributes
Beldring et al. (2002)	Norway	HBV	Daily	Regression with catchment attributes
Parajka et al. (2005a)	Austria	HBV (Semi lumped)	Daily	Regression with catchment Attributes, Similarity concepts, Spatial Proximity methods (Kriging, nearest neighbor)
Merz & Blöschl (2004)	Austria	HBV (lumped)	Daily	Regression with catchment attribute. Similarity concepts Spatial proximity methods (Kriging, nearest neighbor)
Young (2006)	UK	PDM	Daily	Regression with catchment attributes Nearest neighbor approach based on similarity in catchment attributes
Hundecha & Bárdossy (2004)	Rhine basin	HBV	Daily	Regional calibration of parameter of regression function of model parameters and catchment attributes
Vandewiele & Elias (1995)	Belgium	3 parameter water balance model	Monthly	Spatial proximity methods (Kriging, nearest neighbor)

Source: (Merz, et al., 2006)

2.4.1 Regionalization based on spatial proximity

The regionalization based on the spatial proximity assumes that the catchments that are close to each other will have a similar response as the climate and catchment conditions will only

vary smoothly in space. The notion of spatial proximity is by no means trivial as it can be defined in several ways and the choice of method in any particular case is usually not obvious. This can be achieved by delineating the spatially contiguous regions with approximately homogeneous model parameters. The regions are found from an analysis of several gauged catchments and available hydrological information using statistical tools such as cluster analysis, principal component analysis and multiple regression (Nathan & McMahon, 1990). Hydrological information to assist in delineating homogeneous regions usually consists of hydrogeological maps, climate maps, soil and vegetation maps and process indicators such as the seasonality of hydrological processes to establish regional flow duration curves, which comprise a family of regression equations relating the flow of various exceedance percentages with catchment area (Yu & Yang, 2000). The regional flow duration curves can then be used to calibrate model parameters in ungauged catchments. An alternative to homogeneous regions is geostatistical methods, such as kriging. The main strength of kriging is that it is a best linear unbiased estimator (BLUE); best meaning that the mean squared error is a minimum, linear meaning that the estimate is a weighted mean of the data in the area, and unbiased meaning that the mean expected error is zero (Merz & Bloschl, 2004).

2.4.2 Regionalization based on catchment attributes

The analysis of observed hydrological behavior often reveals small scale variability but catchments that are far apart may still be hydrologically similar (Pilgrim, 1983), hence the alternatives to the spatial proximity concepts have been proposed in literature. These concepts are often based on similarity of catchment attributes that are available in both gauged and ungauged catchments. Runoff is not considered as a catchment attribute that will make this group of methods applicable to the ungauged catchment case. Catchment attributes include catchment size, information on topography, land use, geology, elevation, soil characteristics, as well as climate variables such as mean annual precipitation, and are thought of as surrogates of the hydrological processes within a catchment. The rationale of this approach is that catchments with similar attributes may also behave hydrologically similarly (Bloschl, 2005). The catchment attributes can be used in regionalization methods of various structures. The first type of methods uses a distance measure of hydrological similarity which is a function of the differences in catchment attributes of two catchments. The distance measure is zero if the catchment attributes are identical and increases as the attributes get more dissimilar. The distance measure can be used in statistical methods such as cluster analysis, principal component analysis, and classification trees to group the catchments (Nathan & McMahon, 1990). Once the groups are identified, the model parameters can be transferred from an analogue gauged catchment within the same group to the ungauged catchment of interest. The second way of using catchment attributes are regression analyses between model parameters and catchment attributes. Regression relationships are black-box models, although some degree of process reasoning can come in. Due to the availability of catchment attributes in geographic information systems, correlations between model parameters and catchment attributes are widely used in regionalization (Merz & Bloschl, 2004). In multiple regressions, one may encounter the problem of multicollinearity, i.e. when at least one of the attributes is highly

correlated with another attribute or with some linear combination of them. If multicollinearity is present, the regression coefficient can be highly unstable and unreliable (Hirsch et al., 1992). One therefore limits the number of catchment attributes used in the regression, sometimes combining several attributes into an index, which is assumed to be representative of one aspect of the rainfall–runoff relationship (Institute of Hydrology, 1999).

2.5 The role of Remote Sensing, Geographical Information Systems (GIS) and Digital Elevation Model (DEM) in Rainfall-Runoff Modelling

Traditionally, streamflow is directly measured through manual or automated ground-based instruments installed within a monitoring station, and most data used for modelling was from field measurements only. There is wide consensus that such data does not represent the areas larger than the local scale. However, sparse hydrological monitoring networks are not enough on the ground, hence creating problems in many regions, especially developing countries when it comes to data analysis. To overcome the limited reliable hydrology data problem, remote sensing is a suitable way or even the only way to acquire information for data-scarce areas (Randall, 2006).

Remote sensing has been used in many hydrological studies to simulate stream flows in ungauged catchments. One of the studies that is of interest to this research is the works of Muzumara (2011) who carried out a study on how to apply Remote Sensing and a GIS based Soil Water Assessment Tool (SWAT) to estimate river discharge for the basin in order to address the water resource management challenges. The results showed good correlation with observed data after calibration.

Remote sensing is the process of acquiring data/information about objects/substances not in direct contact with the sensor, by gathering its inputs using electromagnetic radiation or acoustical waves that emanate from the targets of interest. An aerial photograph is a common example of a remotely sensed (by camera and film, or now digital) product.

The sun is a source of energy or radiation, which provides a very convenient source of energy for remote sensing. The sun's energy is either reflected, as it is for visible wavelengths, or absorbed and then reemitted, as it is for thermal infrared wavelengths. There are two main types of remote sensing, Passive remote sensing and Active remote sensing as shown in Figure 3.

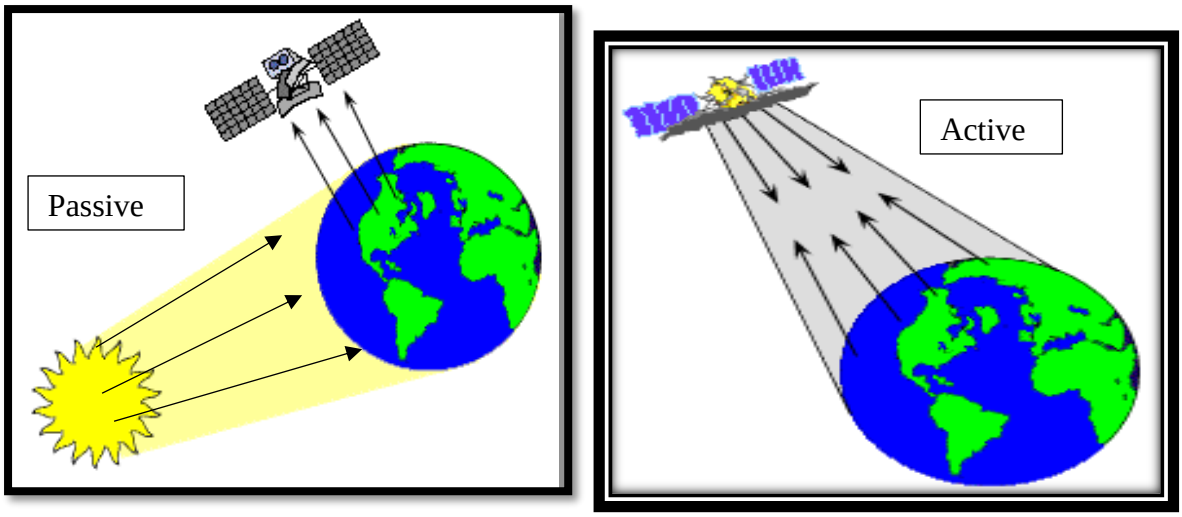

Figure 3. Remote Sensing Processes (source; Randall, 2006)

Passive sensors detect natural radiation that is emitted or reflected by the object or surrounding area being observed. Reflected sunlight is the most common source of radiation measured by passive sensors. Examples of passive remote sensors include film photography, infrared, and radiometers.

Active remote sensing, on the other hand, emits energy in order to scan objects and areas whereupon a sensor then detects and measures the radiation that is reflected or backscattered from the target. RADAR is an example of active remote sensing where the time delay between emission and return is measured, establishing the location, height, speeds and direction of an object.

2.5.1 Types of Remote Sensing System

Remote sensing can be split in five general types namely: Visual remote sensing system, Optical Remote Sensing, Infrared Remote Sensing, Microwave Remote Sensing and Radar Remote Sensing (Elachi & Zyl, 2006).

The human visual system is an example of a remote sensing system in the general sense. The sensors in this example are the two types of photosensitive cells, known as the cones and the rods, at the retina of the eyes. The cones are responsible for color vision. There are three types of cones, each being sensitive to one of the red, green, and blue regions of the visible spectrum. Thus, it is not coincidental that the modern computer display monitors make use of the same three primary colors to generate a multitude of colors for displaying color images. The cones are insensitive under low light illumination condition, when their jobs are taken over by the rods. The rods are sensitive only to the total light intensity. Hence, everything appears in shades of grey when there is insufficient light. As the objects/events being observed are located far away from the eyes, the information needs a carrier to travel from the object to the eyes. In this case, the information carried is the visible light, a part of the electromagnetic spectrum. The

objects reflect/scatter the ambient light falling onto them. Part of the scattered light is intercepted by the eyes, forming an image on the retina after passing through the optical system of the eyes. The signals generated at the retina are carried via the nerve fibers to the brain, the central processing unit (CPU) of the visual system as shown in Figure 4 (Lillesand, et al., 2004).

These signals are processed and interpreted at the brain, with the aid of previous experiences. The visual system is an example of a "Passive Remote Sensing" system which depends on an external source of energy to operate. It's a known fact that this system does not work in darkness.

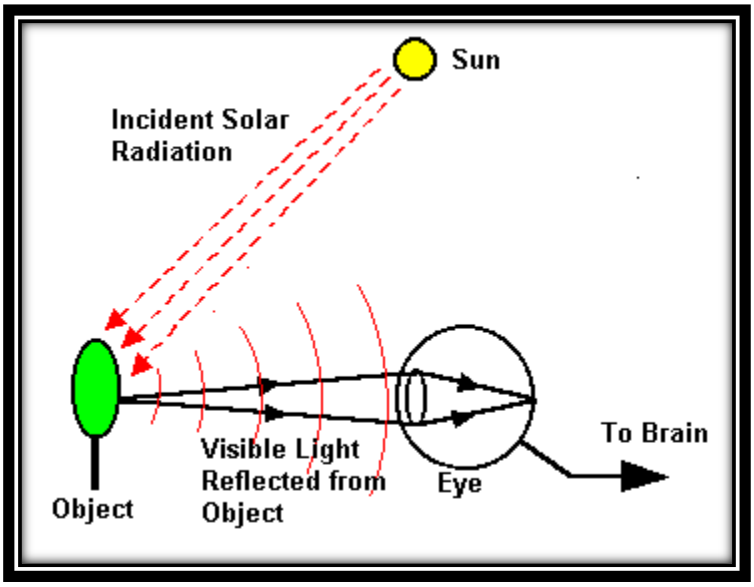

Figure 4. Visual Remote Sensing (Source: Lillesand, et al., 2004)

In Optical Remote Sensing, optical sensors detect solar radiation reflected or scattered from the earth, forming images resembling photographs taken by a camera high up in space. The wavelength region usually extends from the visible and near infrared (VNIR) to the short-wave infrared (SWIR). Different materials such as water, soil, vegetation, buildings and roads reflect visible and infrared light in different ways. They have different colours and brightness when seen under the sun. The interpretations of optical images require the knowledge of the spectral reflectance signatures of the various materials (natural or man-made) covering the surface of the earth.

Infrared remote sensing makes use of infrared sensors to detect infrared radiation emitted from the Earth's surface. The middle-wave infrared (MWIR) and long-wave infrared (LWIR) are within the thermal infrared region. These radiations are emitted from warm objects such as the Earth's surface. They are used in satellite remote sensing for measurements of the earth's land and sea surface temperature. Thermal infrared remote sensing is also often used for detection of forest fires, volcanoes, and oil.

There are some remote sensing satellites which carry passive or active microwave sensors. The active sensors emit pulses of microwave radiation to illuminate the areas to be imaged. Images

of the earth surface are formed by measuring the microwave energy scattered by the ground or sea back to the sensors. These satellites carry their own "flashlight" emitting microwaves to illuminate their targets. The images can thus be acquired day and night. Microwaves have an additional advantage as they can penetrate clouds. Images can be acquired even when there are clouds covering the earth surface. A microwave imaging system which can produce high resolution image of the Earth is the synthetic aperture radar (SAR). Electromagnetic radiation in the microwave wavelength region is used in remote sensing to provide useful information about the Earth's atmosphere, land and ocean. When microwaves strike a surface, the proportion of energy scattered back to the sensor depends on many factors:

- Physical factors such as the dielectric constant of the surface materials which also depends strongly on the moisture content.
- Geometric factors such as surface roughness, slopes, orientation of the objects relative to the radar beam direction.
- The types of landcover (soil, vegetation or man-made objects).
- Microwave frequency, polarization and incident angle.

Using radar, geographers can effectively map out the terrain of a territory. Radar works by sending out radio signals, and then waiting for them to bounce off the ground and return. By measuring the amount of time, it takes for the signals to return, it is possible to create a very accurate topographic map, an example of the radar antenna is shown in Figure 5.

An important advantage to using radar is that it can penetrate thick clouds and moisture. This allows scientists to accurately map areas such as rain forests, which are otherwise too obscured by clouds and rain. Imaging radar systems are versatile sources of remotely sensed images, providing day night, all-weather imaging capability. Radar images are used to map landforms and geologic structure, soil types, vegetation and crops, and ice and oil slicks on the ocean surface.

Figure 5. Radar Antenna (Lillesand, et al., 2004)

2.5.2 Remote Sensing applications in Hydrology

Hydrology is the study of water on the Earth's surface, whether flowing above ground, frozen in ice or snow, or retained by soil. Hydrology is inherently related to many other applications of remote sensing, particularly forestry, agriculture and land cover, since water is a vital component in each of these disciplines. Most hydrological processes are dynamic, not only between years, but also within and between seasons, and therefore require frequent observations. Remote sensing offers a synoptic view of the spatial distribution and dynamics of hydrological phenomena, often unattainable by traditional ground surveys. Radar has brought a new dimension to hydrological studies with its active sensing capabilities, allowing the time window of image acquisition to include inclement weather conditions or seasonal or diurnal darkness.

Accurate measurement of precipitation is a continuing goal in meteorological research and a continuing need in hydrology which depends greatly on these data for modelling. Ground-based radar is probably the most accurate method of determining real precipitation in use today. Satellite images from GOES (The Geostationary Operational Environmental Satellite system), NOAA (National Oceanic and Atmospheric Administration), TIROS-N (Television Infrared Observation Satellite), TRMM (Tropical Rainfall Measuring Mission) and NIMBUS opened a whole new world of data clouds and frontal systems. Figure 8 shows Satellite data in the land surface hydrological cycle coupled with the use of remote sensing techniques

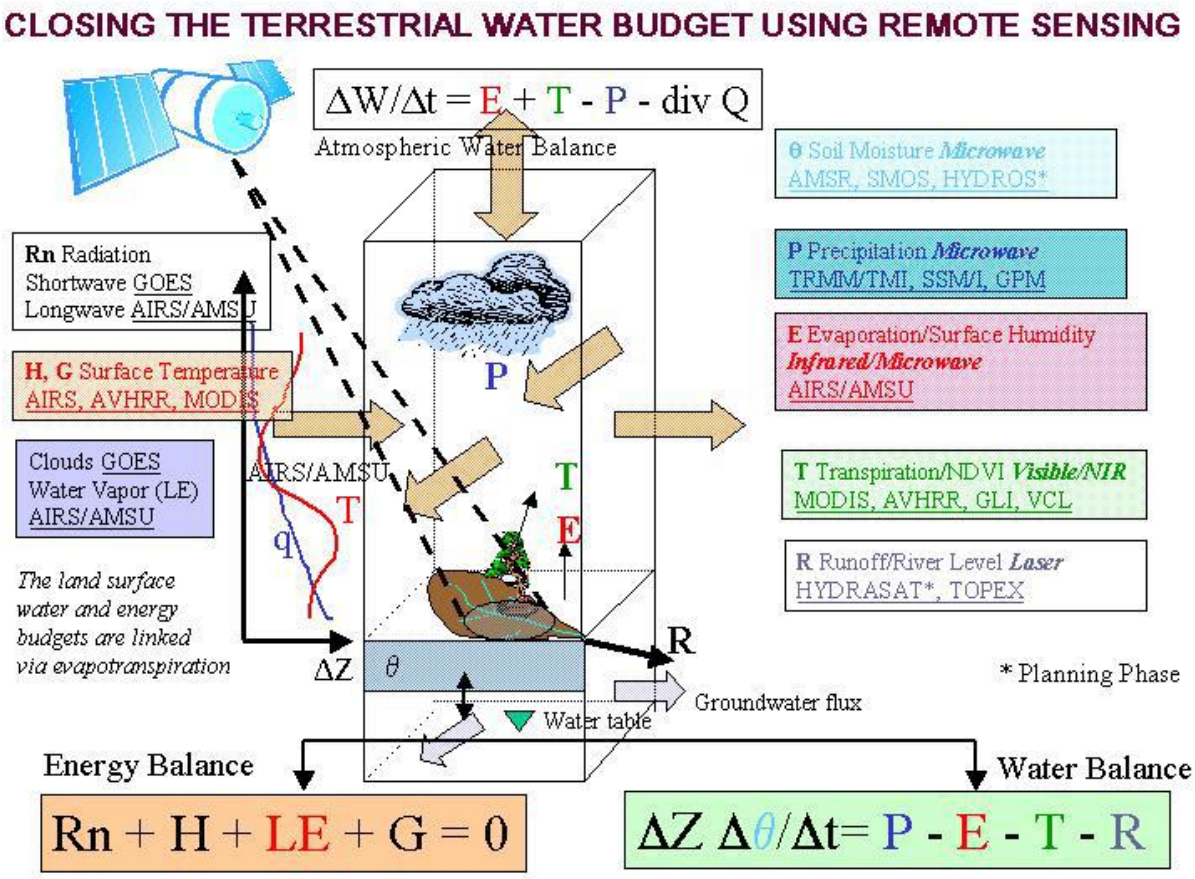

Figure 6. Satellite Data in the Land Surface hydrological cycle, Source: (Elachi & Zyl, 2006).

It can be noted that, one can hardly find any rainfall-runoff models that do not use RS and GIS data. A lot of research conducted has introduced and confirmed that RS and GIS are powerful tools in rainfall-runoff modelling. Schultz, 1996, contributed to the introduction of different applications of RS in Hydrology. Dataset for ungauged catchments can be obtained for free from public domain satellite data such as SRTM, TRMM (Rabus, et al., 2003) for DEM generation and rainfall estimation. SRTM (Shuttle Radar Topography Mission) with resolution of 30m or 90m accuracy can be found at:

http://www2.jpl.nasa.gov/srtm/.

http://srtm.csi.cgiar.org/SELECTION/inputCoord.asp

http://earthexplorer.usgs.gov/

For the sake of this study the DEM tiles were downloaded from http://earthexplorer.usgs.gov/. while the TRMM rainfall data was downloaded from http://disc2.nascom.nasa.gov/Giovanni/tovas/TRMM_V6.3B42.2.shtml. The GIS processing of the DEM was done using QGIS, which is an open source GIS software with the help of hydrological plugins tools. QGIS can be downloaded at www.qgis.org. The selection of QGIS was based on multiple factors including: its compatibility with multiple operating systems

(Microsoft Windows, Macintosh, Linux etc.), an uncluttered user-friendly interface, easy plugin-development functionality, support of wide range of data formats, an active developer community to support state-of-the-art software and hardware developments. It is comprised of four major subsystems: input/capture; management; manipulation/analysis; and output/ display. The data input/capture subsystem, provides operational functions for reading, collecting, capturing, and querying geospatial data. The data management subsystem organizes and stores spatial data and their attributes to enable efficient query and quick retrieval for display, processing, and analysis. It also manages the modification and update of existing databases through editing tools. The manipulation and analysis subsystem execute the transformation of data from one form to another depending on model applications. The data display subsystem provides visual aids for quick interpretation of geospatial data in the form of diagrams, maps, or tables as well as data output providing access to the analyzed data in one of the several supported file formats.

2.6. RS Minerve Hydrological Modelling Software

RS MINERVE is a software for the simulation of free surface run-off flow formation and propagation. It models complex hydrological and hydraulic networks either as a lumped model or a semi-distributed conceptual scheme. In addition to hydrological processes such as snowmelt, glacier melt, surface and underground flow, hydraulic control elements (e.g. gates, spillways, diversions, junctions, turbines and pumps) are also included.

The global analysis of a hydrologic-hydraulic network is essential in numerous decision-making situations such as the management or planning of water resources, the optimization of hydropower plant operations, the design and regulation of spillways or the development of appropriate flood protection concepts. RS MINERVE makes such analyses accessible to a broad public through its user-friendly interface and its valuable possibilities. In addition, it can be adopted various specific needs or issues.

RS MINERVE contains different hydrological models for rainfall-runoff, such as GSM, SOCONT, SAC-SMA, GR4J and HBV. The combination of hydraulic structure models (reservoirs, turbines, spillways) can also reproduce complex hydropower schemes. In addition, a hydropower model computes the net height and the linear pressure losses, providing energy production values and total income based on the turbine performance and on the sale price of energy. A consumption model calculates water deficits for consumptive uses of cities, industries and/or agriculture. A structure efficiency model computes discharge loss in a structure such a canal or a pipe by considering a simple efficiency coefficient.

The RS MINERVE was developed by the CREALP and HydroCosmos SA, with the collaboration with the Universitat Politècnica de València (UPV). It has also been used since 2011 in numerous projects in Switzerland, Spain, Peru, Brazil, Uganda and theses (Hernandez, et al., 2017).

2.6.1 Overview of the RS MINERVE Hydrological models for rainfall-runoff Simulation

RS MINERVE contains different hydrological models for rainfall-runoff, such as GSM, SOCONT, SAC-SMA, GR4J and HBV.

The Snow-GSM model (Figure 7) is composed of two sub-models which simulate the transient evolution of the snow pack (accumulation and melt) as a function of the temperature (T) and precipitation (P) producing an equivalent precipitation (Peq) which can be used as an input variable by the SAC-SMA or GR4J model.

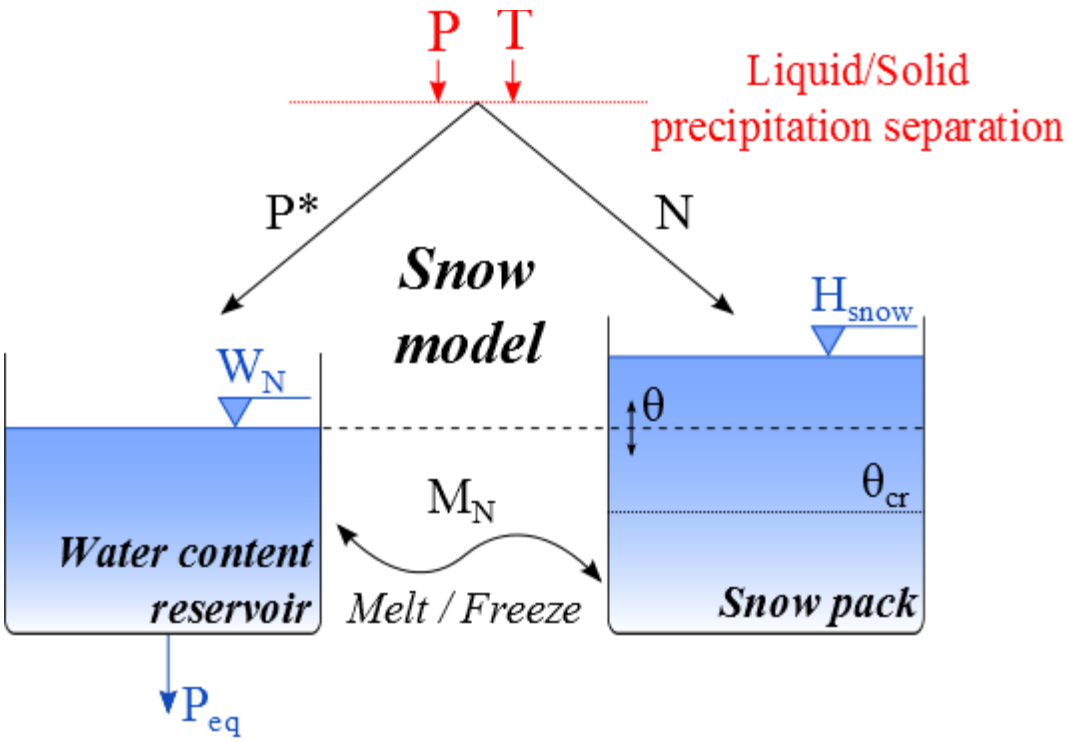

Figure 7. Snow-GSM Modell

The SWMM (Storm Water Management Model) model Figure 8, presented hereafter was developed by Metcalf and Eddy (1971).

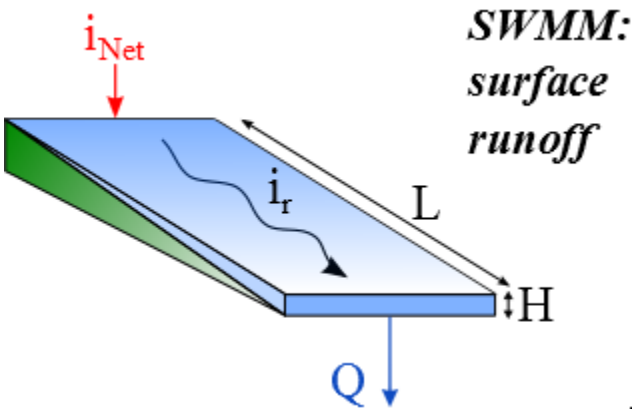

Figure 8. SWMM Model

The GSM model (Figure 9) is composed of 5 sub-models, two corresponding to the Snow-GSM model and the other three corresponding to the glacier model. The hereafter present model allows an easy construction of this kind of composition.

From the inputs of precipitation (P) and temperature (T), the snow model creates an equivalent precipitation (Peq) which is transferred to the glacier model. The same accounts for the height of the snow (Hsnow) and the temperature (T).

In the glacier model the equivalent precipitation is transferred to the linear snow reservoir (Rsn) and finally to the outlet of the sub-catchment (Qsnow). Besides, the sub-model of the glacier melt creates a flow when the height of snow is zero (Hsnow=0). This glacier flow (PeqGL) is transferred to the linear glacier reservoir (Rgl) and the resulting flow (Qglacier) to the outlet of the sub-catchment. The final flow (Qtot) produced by the sub-catchment is the addition of the two flows (Qglacier and Qsnow).

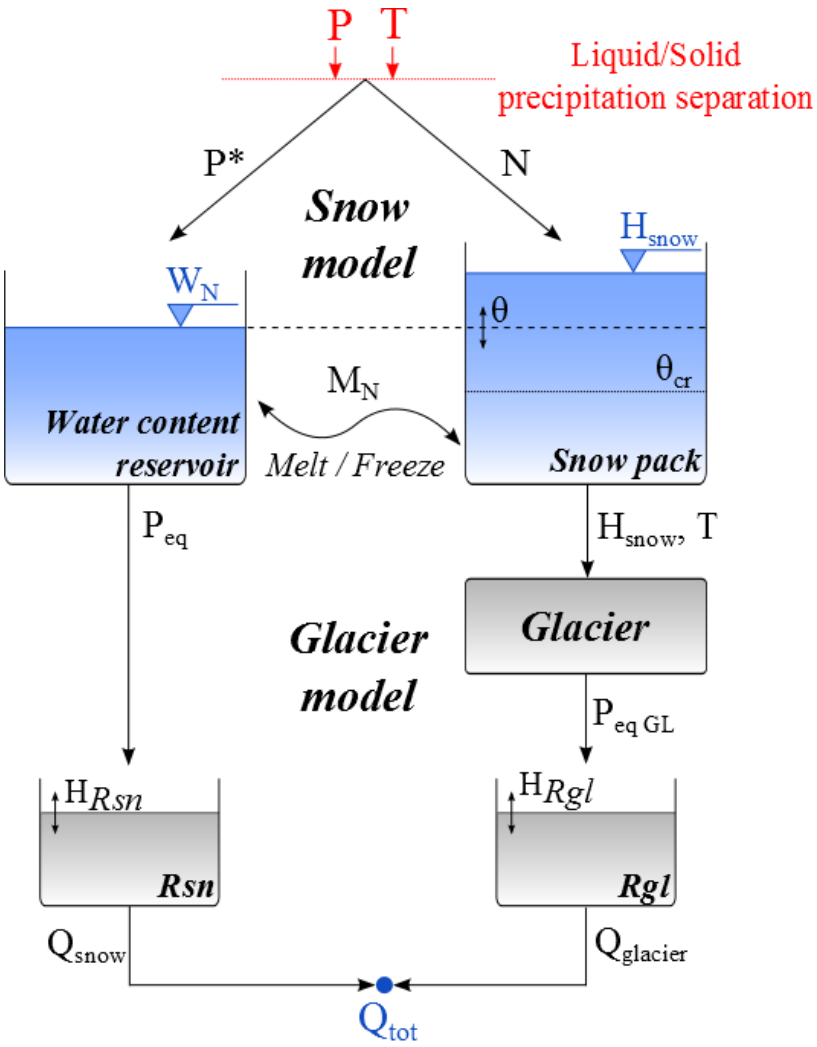

Figure 9. GSM Model

In the SOCONT model (Figure 10), the Snow-GSM model simulates the transient evolution of the snow pack (melt and accumulation) as a function of the temperature (T) and the precipitation (P), thus providing an equivalent precipitation (Peq) that is used as input by the GR3 model. The GR3 model also takes into account the potential evapotranspiration (ETP) and provides the net intensity to the SWMM model.

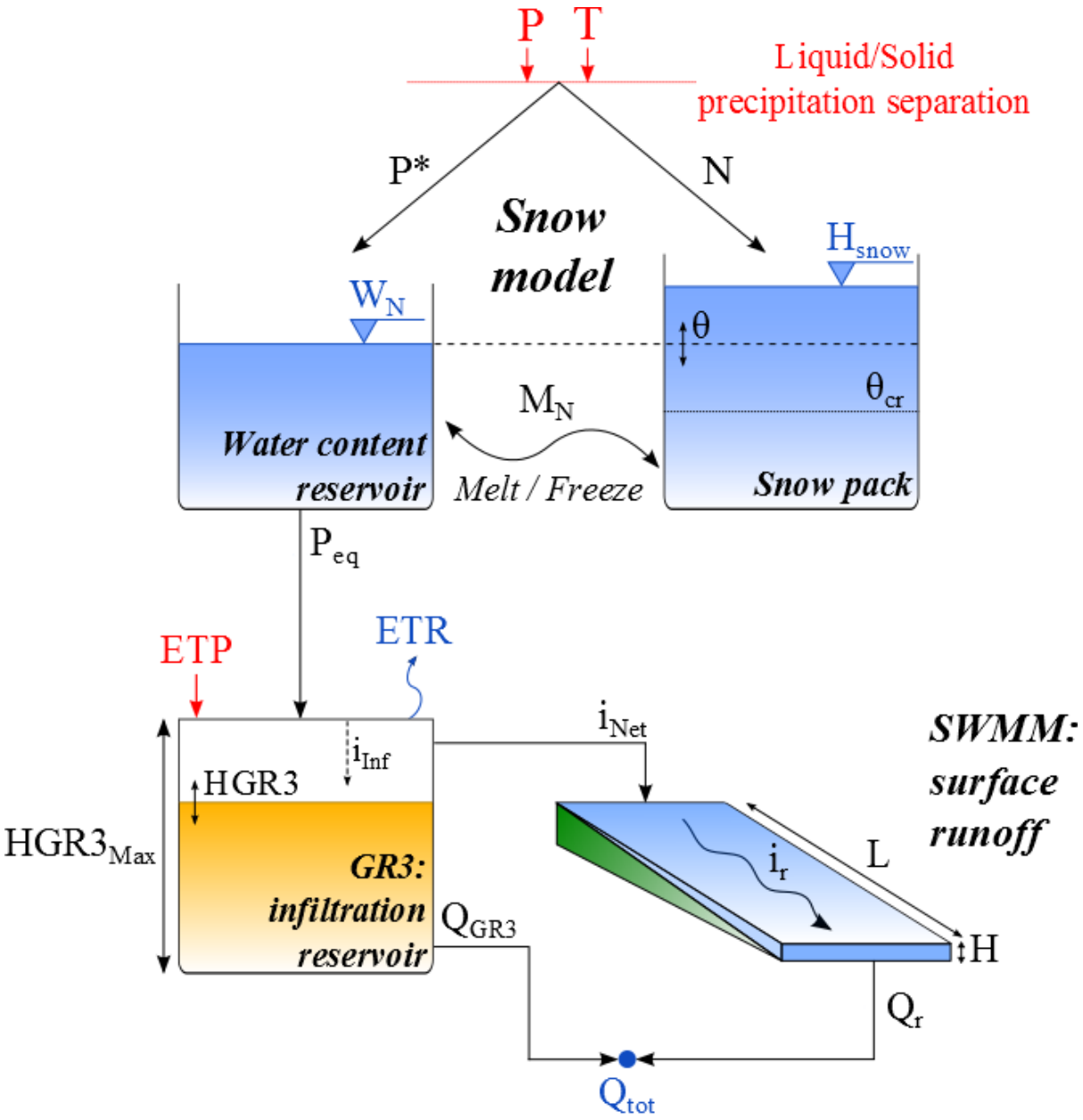

Figure 10. SOCONT Model

The integrated rainfall-runoff model HBV (Bergström, 1976, 1992) is composed of a snow function, a humidity reservoir and two (upper and lower) soil storage reservoirs. The structure of the implemented model is presented in the Figure 11

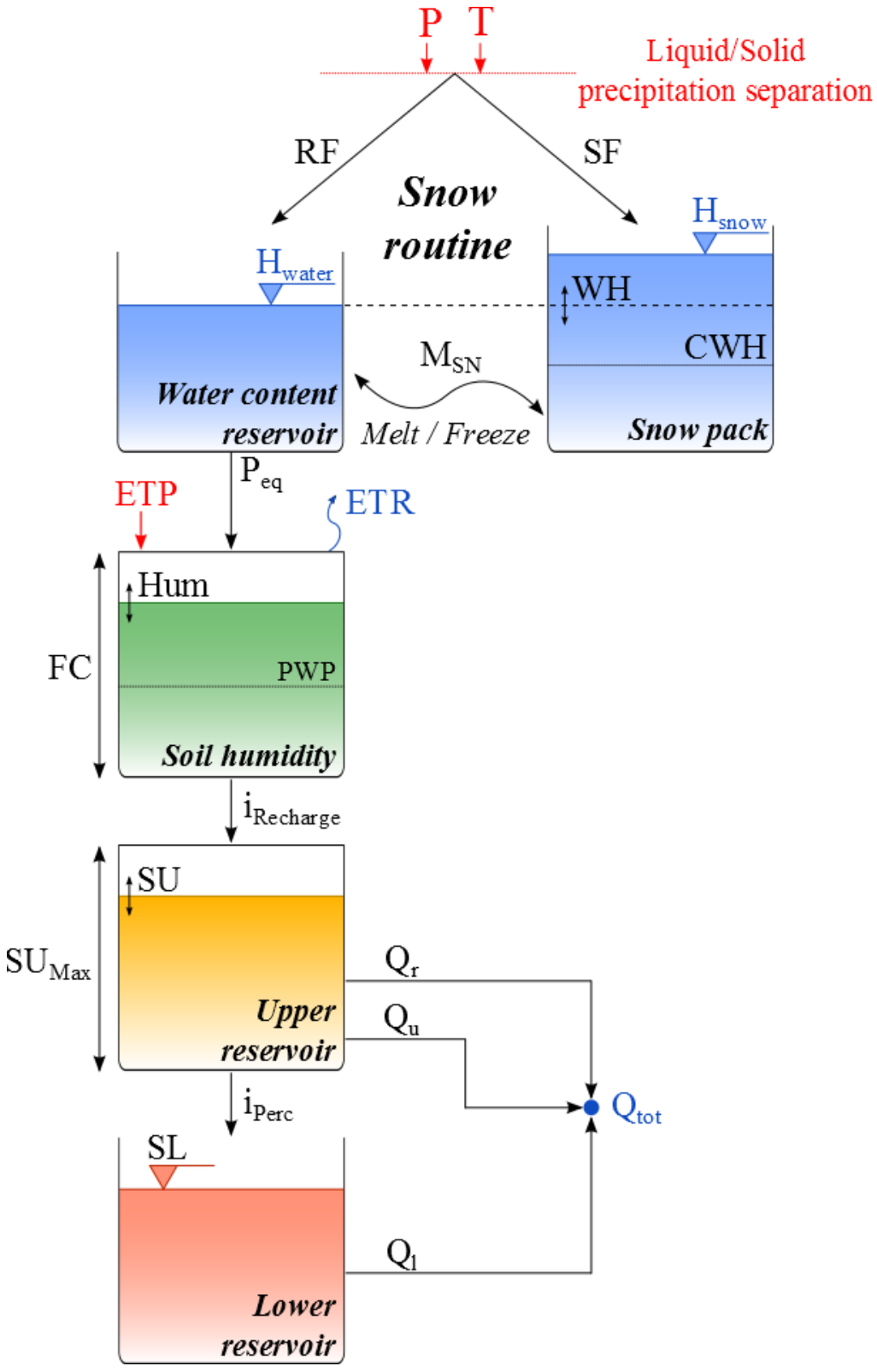

Figure. 11 HBV Model

The GR4J model is a global hydrological model with four parameters developed by Perrin et al. (2003). It is an empirical model (Figure 12), but its structure is like the conceptual models. It considers the humidity and contains two reservoirs (production and routing). Unit hydrographs are also associated for the hydrological behavior of the basin

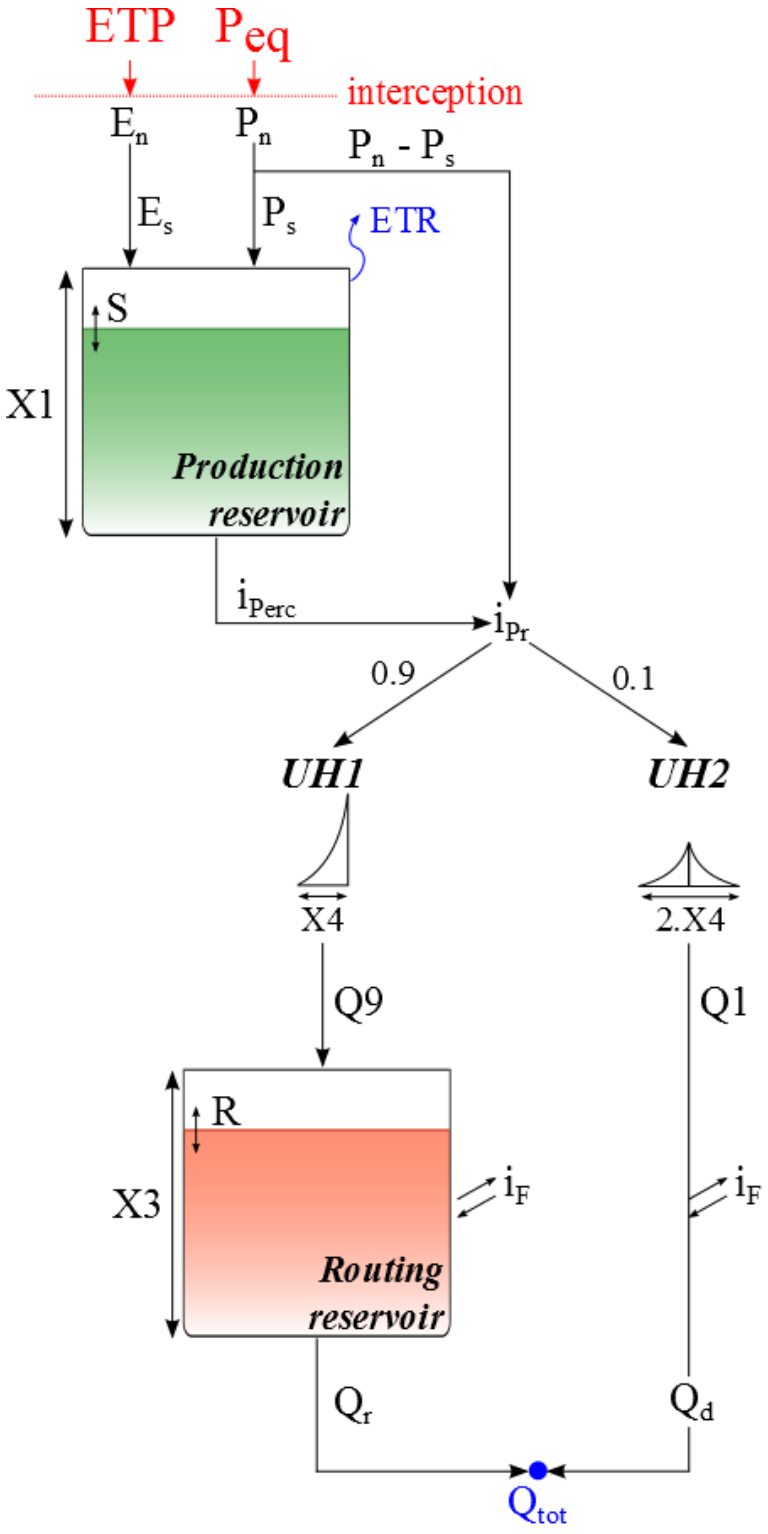

Figure 12. GR4J Model

2.6.2 Governing Equations and initial Parameters of HBV Model in RS MINERVE

The integrated rainfall-runoff model HBV (Bergström, 1976, 1992) is composed of a snow function, a humidity reservoir and two (upper and lower) soil storage reservoirs. The structure of the implemented model is presented in the Figure 11 and Figure 13.

The precipitation is first divided into snowfall (SF) and rainfall (RF) as a function of the temperature, equations H1 to H3 (an abbreviation for letter "H" has been used to denote governing equations relating to HBV Model). If the observed temperature is lower than TT-TTInt/2, only solid snowfall is produced. If the temperature is higher than TT+TTInt/2, only rainfall is produced. If the observed temperature is found between these values, both rainfall and snowfall are produced.

$$RF=\alpha \cdot P \qquad \text{Equation H1}$$

$$SF=(1-\alpha)\cdot P \qquad \text{Equation H2}$$

$$\alpha=0 \; if \; T<TT-TTInt/2 \alpha=T-(TT-TTInt/2) \; TTInt \; if \; TT-TTInt/2<T<TT+TTInt/2 \alpha=1 \; if \; T>TT+TTInt/2 \qquad \text{Equation H3}$$

with RF: rainfall [L/T]; α: separation factor; P: precipitation [L/T]; SF: snowfall [L/T]; T: temperature [°C]; TT: threshold temperature for rain/snow [°C]; TTInt: temperature interval for rain/snow mixing [°C].

The snowfall (SF) is used as input for the snow pack, varying its content as a function of melt or freezing. The snowmelt calculation is performed as follows:

$$Msn=CFMax\cdot(T-TTSM) \; if \; T>TTSM Msn=CFR\cdot CFMax\cdot(T-TTSM) \; if \; T\leq TTSM \qquad \text{Equation H4}$$

$$dHsnow/dt=SF-Msn Msn\leq SF+Hsnow/dt Msn\geq -Hwater/dt \qquad \text{Equation H5}$$

with Msn: snowmelt or freezing [L/T]; CFMax: degree-day melting factor [L/T/°C]; CFR: refreezing factor [-]; TTSM: critical snowmelt temperature [°C]; Hsnow: snow height [L]; Hwater: water content [L]; dt: time step [T].

The equivalent precipitation (Peq) is produced by the water content of the snow (equations H.6 to H.8):

$$WH=Hwater/Hsnow \qquad \text{Equation H6}$$

$$Peq=RF+Hwater/dt \; if \; Hsnow=0 Peq=0 \; if \; Hsnow>0 \; et \; WH\leq CWH Peq=(WH-CWH)\cdot Hsnow/dt \; if \; Hsnow>0 \; et \; WH>CWH \qquad \text{Equation H7}$$

$dHwater/dt=RF+Msn-Peq$ Equation H8

with WH: relative water content in the snow pack [-]; CWH: critical relative water content in the snow pack [-]; Peq: equivalent precipitation [L/T].

The calculation of the recharge is carried out depending on a model parameter Beta, as presented in equation H.9. ETR is calculated as shown in equation H.10. Finally, the humidity of the soil (Hum) is performed taking into account the input (Equivalent precipitation, Peq) and outputs (Recharge intensity and ETR) as presented in equation H.11. Additionally, and based on Seibert (1997), parameter PWP is a rate related to parameter FC. Thus, the height of the soil permanent wilting point threshold is calculated multiplying PWP by FC.

iRecharge=$(HumFC)Beta \cdot Peq$ Equation H9

$ETR=ETP \cdot Hum(PWP \cdot \mathrm{FC})\ if\ Hum<(PWP \cdot \mathrm{FC})ETR=ETP\ if\ Hum\geq(PWP \cdot \mathrm{FC})$ Equation H10

$dHum/dt=(Peq-i\mathrm{Recharge})-ETR\ Hum\geq 0$ Equation H11

with iRecharge: Reservoirs recharge intensity [L/T] ; Hum: Humidity [L]; FC: Maximum soil storage capacity [L] ; Beta: Model parameter (shape coefficient) [-]; Peq: Equivalent precipitation [L/T]; ETR: Evapotranspiration [L/T] ; ETP: Potential evapotranspiration [L/T] ; PWP: Soil permanent wilting point threshold [-].

Then, near surface (or run-off) flow is calculated depending on the water level in the Upper reservoir (SU) and its threshold, as well as on a flow storage coefficient Kr.

$Qr=Kr \cdot (SU-SUMax) \cdot A\ if\ SU>SUMaxQr=0\ if\ SU\leq SUMax$ Equation H12

with Qr: Near surface flow (or run-off flow) [L3/T]; Kr: Near surface flow storage coefficient [1/T]; SU: Upper reservoir water level [L]; SUMax: Upper reservoir water level threshold [L]; A: Basin surface [L2].

The Upper reservoir (or interflow reservoir), corresponding to the upper soil storage and producing the interflow, is computed as follows:

$dSU/dt=i\mathrm{Recharge}-(Kperc+Ku) \cdot SU-Qr/ASU\geq 0$ Equation H13 (H.13)

iPerc=$Kperc \cdot SU$ Equation H14

$Qu=Ku \cdot SU \cdot A$ Equation H15

with Kperc: Percolation storage coefficient [1/T] ; Ku: Interflow storage coefficient [1/T] ; iPerc: Percolation intensity [L/T] ; Qu: Interflow [L3/T].

Afterwards, the lower reservoir (or baseflow reservoir), corresponding to the lower soil storage, is calculated as presented in equations H.16 and H.17

$dSL/dt = i\text{Perc} - Kl \cdot SL \quad SL \geq 0$ Equation H16

$Ql = Kl \cdot SL \cdot A$ Equation H17

with SL: Lower reservoir water level [L]; Kl: Baseflow storage coefficient [1/T]; Ql: Baseflow [L3/T].

And finally the total outflow is:

$Qtot = Qr + Qu + Ql$ Equation H18

with Qtot: Total outflow [L3/T].

The initial conditions associated to this model are HsnowIni, WHIni, HumIni, SUIni and SLIni. The parameters to adjust are CFMax, CFR, CWH, TT, TTInt, TTSM, Beta, FC, PWP, SUmax, Kr, Ku, Kl and Kperc. The parameter A is supposed to be constant. Table 3 shows a list of Parameters and initial conditions for the HBV Model

The model inputs are the precipitation (P), the temperature (T) and the potential evapotranspiration (ETP). The output is the total discharge at the model outlet (Qtot).

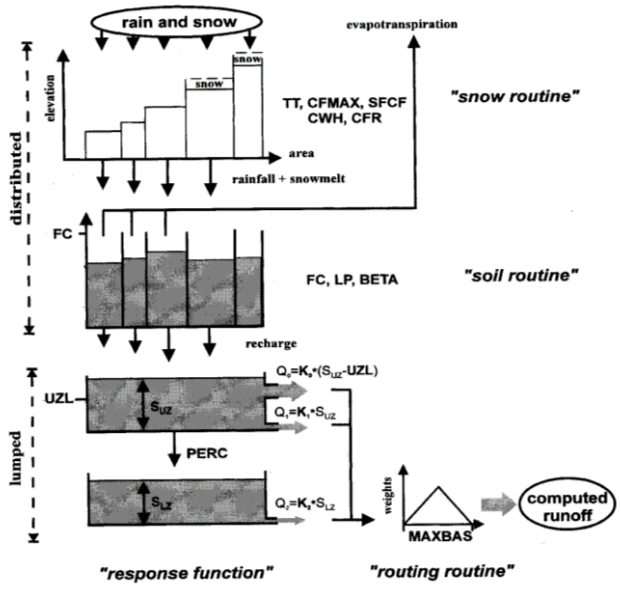

Figure 13. Structure of the HBV Mode (Seibert, 2000)

Table 3. List of Parameters and initial conditions for the HBV Model

Object	Name	Units	Description	Regular Range
HBV	A	m2	Surface of the basin	>0
	CFMax	mm/°C/day	Melting factor	0.5 to 20
	CFR	-	Refreezing factor	0.05
	CWH	-	Critical relative water content of the snow pack	0.1
	TT	°C	Threshold temperature of rain/snow	0 to 3
	TTInt	°C	Temperature interval for rain/snow mixing	0 to 3
	TTSM	°C	Threshold temperature for snow melt	0
	Beta	-	Model parameter (shape coefficient)	1 to 5
	FC	m	Maximum soil storage capacity	0.050 to 0.65
	PWP	-	Soil permanent wilting point threshold	0.030 to 1
	SUMax	m	Upper reservoir water level threshold	0 to 0.10
	Kr	1/d	Near surface flow storage coefficient	0.05 to 0.5
	Ku	1/d	Interflow storage coefficient	0.01 to 0.4
	Kl	1/d	Baseflow storage coefficient	0 to 0.15
	Kperc	1/d	Percolation storage coefficient	0 to 0.8

	HsnowIni	m	Initial snow height	-
	WHIni	-	Initial relative water content in the snow pack	-
	HumIni	m	Initial humidity	-
	SUIni	m	Initial upper reservoir water level	-
	SLIni	m	Initial lower reservoir water level	-

Source: **(Hernandez, et al., 2017)**

2.6.3 Model Performance indicators in RS MINERVE

The Comparator object embedded in the RS Minerve software provides seven indicators values used to evaluate the model performance, these are presented in the sections below. The letters "IND" has been used to represent the governing equations for each of the model performance indicator that RS Minerve uses.

2.6.3.1 Nash coefficient

The Nash-Sutcliffe criteria (Nash & Sutcliffe, 1970) is used to assess the predictive power of hydrological models (Ajami et al., 2004; Viviroli et al., 2009; García Hernández et al., 2011). It is defined as presented in Eq. IND.1.

$Nash=1-\Sigma(Qsim,t-Qref,t)2tft=ti\Sigma(Qref,t-Qref)2tft=ti$ Equation IND 1

with Nash: Nash-Sutcliffe model efficiency coefficient [-]; Qsim,t: simulated discharge at time t [L3/T]; Qref,t : observed discharge at time t [L3/T]; ref: average observed discharge for the considered period [L3/T].

The Nash coefficient varies from -∞ to 1, with 1 representing the best performance of the model and zero the below performance, it assumes the average of all the observations at each time step.

2.6.3.2 Nash coefficient for logarithm values

The Nash-Sutcliffe coefficient for logarithm flow values (Nash-ln) is used to assess the hydrological models performance for low flows (Nobrega, et al., 2011). It is defined as presented in Eq. IND.2.

Nash-ln=1−Σ(ln($Qsim,t$)−ln($Qref,t$))2$tft=ti$Σ(ln($Qref,t$)−ln($Qref$))2$tft=ti$

Equation IND2

with Nash-ln: Nash-Sutcliffe coefficient for log values [-].

It varies from -∞ to 1, with 1 representing the best performance of the model.

2.6.3.3 Pearson Correlation Coefficient

The Pearson correlation coefficient shows the covariability of the simulated and observed discharges without penalising for bias (AghaKouchak and Habib, 2010; Wang et al., 2011). It is defined as presented in Eq. IND.3.

$Pearson$=Σ($Qsim,t-Qsim$)·($Qref,t-Qref$)$tft=ti$√Σ($Qsim,t-Qsim$)2$tft=ti$·Σ($Qref,t-Qref$)2$tft=ti$

Equation IND3

with Pearson: Pearson Correlation Coefficient [-]; sim: average simulated discharge for the considered period [L3/T].

It varies from -1 to 1, with 1 representing the best performance of the model.

2.6.3.4. Kling-Gupta Efficiency

The Kling-Gupta efficiency (Gupta, et al., 2009) provides an indicator which facilitates the global analysis based on different components (correlation, bias and variability) for hydrological modelling issues.

Kling et al. (2012) proposed a revised version of this indicator, to ensure that the bias and variability ratios are not cross-correlated. This update is proposed as indicator in RS MINERVE (Eq. IND.4):

KGE'=1−√(r−1)2+(β−1)2+(γ−1)2

Equation IND4

with KGE': modified KGE-statistic [-];r: correlation coefficient between simulated and reference values [-]; β: ratio between the mean of the simulated values and the mean of the reference ones [-] ; γ: variability ratio, i.e., ratio between the coefficient of variation of the simulated values and the coefficient of variation of the reference ones [-].

It varies from 0 to 1, with 1 representing the best performance.

2.6.3.5 Bias Score

The Bias Score (BS) is a symmetric estimation of the match between the average simulation and average observation (Wang, et al., 2011). It is defined as presented in Eq. IND.5.

BS=1−[max($QsimQref$,$QrefQsim$)−1]2 Equation IND5

with BS: Bias Score [-].

It varies from 0 to 1, with 1 representing the best performance of the model.

2.6.3.6 Relative Root Mean Square Error

The Relative Root Mean Square Error (RRMSE) is defined as the RMSE normalized to the mean of the observed values (Feyen, et al., 2000) and is presented in Eq. IND.6.

$RRMSE$=√Σ($Qsim$,t−$Qref$,t)2tft=$tinQref$ Equation IND6

with RRMSE: relative RMSE [-]; n: number of values [-].

It varies from 0 to +∞. The smaller RRMSE, the better the model performance is.

2.6.3.7. Relative Volume Bias

The Relative Volume Bias (RVB), sometimes called differently, corresponds in this case to the relative error between the simulated and the observed volumes during the studied period (Ajami, et al., 2004, AghaKouchak & Habib, 2010,and Moriasi, et al., 2007) according to Eq. IND.7.

RVB=Σ($Qsim$,t−$Qref$,t)tft=tiΣ($Qref$,t)tft=ti Equation IND7

with RVB: relative volume bias between forecast and observation for the considered period [-].

The RVB varies from -1 to +∞. An index near to zero indicates a good performance of the simulation. Negative values are returned when simulated discharge is, in average, smaller than the average of the observed discharge (deficit model), while positive values mean the opposite (overage model).

2.6. 3.8. Normalized Peak Error

The Normalized Peak Error (NPE) indicates the relative error between the simulated and the observed flow peaks (Ajami, et al., 2004 and Gabellani, et al., 2007). It is computed according to equations IND.8 TO IND.10.

$NPE=S\max-R\max R\max$ Equation IND8

$S\max=\vee t=titfQsim,t$ Equation IND9

$R\max=\vee t=titfQref,t$ Equation IND10

with NPE: relative error between simulated and observed peak discharge [-]; Smax : maximum simulated discharge for the studied period [L3/T]: Rmax : maximum observed discharge for the studied period [L3/T].

The NPE varies from -1 to +∞. Negative values are returned when simulated peak discharge is below the observed one, while positive values mean the opposite. Values near to zero indicate a good performance of simulated peaks regarding observed ones.

It should be noted that this indicator is computed over the entire simulation period and the absolute maximum of the simulated and the observed peaks are considered. This indicator should therefore be used with care when simulating over long periods of time.

2.6.4 Model Calibration in RS MINERVE

The RS MINERVE has a module Calibrator for calibrating the parameters of the hydrological model. This module uses an objective function defined by the user and different algorithms to solve it. The first algorithm, the Shuffled Complex Evolution – University of Arizona (SCE-UA), is a global optimization method (Duan, et al., 1994) based on a synthesis of the best features from several existing algorithms, including the genetic algorithm, and introduces the concept of complex information exchange, so-called complex shuffling. The SCE-UA method was designed for solving problems encountered in conceptual watershed model calibration (Ajami, et al., 2004), but has also been satisfyingly used in water resources management (Wang, et al., 2010).

The second algorithm is a variation of the Adaptive Markov Chain Monte Carlo, used since it can be interesting for solving complex problems in high dimensional spaces (Liu, 2001). It has been modified to an Uniform Adaptative Monte Carlo (UAMC) in RS MINERVE to adjust the solution space after a defined group of simulations up to the convergence of the optimization. Variations of the Monte Carlo method have been used in hydrological problem parameterization and optimization (Jeremiah, et al., 2012).

The third and last algorithm used in RS MINERVE is the Coupled Latin Hypercube and Rosenbrock (CLHR) It couples the Latin Hypercube algorithm (McKay, et al., 1979) with the Rosenbrock algorithm (Rosenbrock, 1960), generating a powerful tool for optimisation of complex problems. The latin hypercube algorithm has been used in hydrology for sampling the

initial parameter space, combined the with other methods (Kamali, et al., 2013). Rosenbrock algorithm has been also used for hydrological parameters optimisation or optimisation of numerical functions (Kang, et al., 2011).

CHAPTER 3: DESCRIPTION OF THE STUDY AREA

3.1 Location

Kariba Lower catchment is located between Longitudes of 15°S and 21°S, and Latitudes of 25°E and 32° E, in Kariba catchment, between Zambia and Zimbabwe. Kariba lower catchment has a total area of approximate 166,000 km^2 and lies between 382 and 1577 m above sea level (Figure 14 and 15). It comprises Lake Kariba which is the largest man-made lake in Zambezi with 5,580 km^2 and 64.8 km^3 as surface area and live storage at full supply level (FSL) respectively.

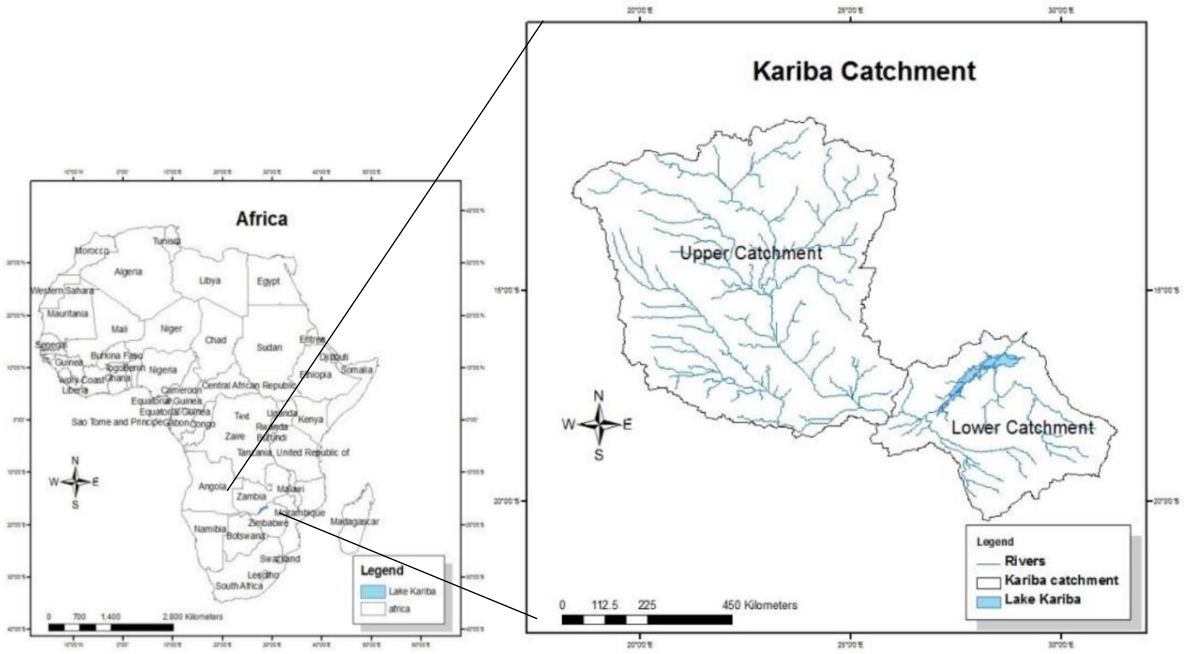

Figure 14. Lake Kariba Lower Catchment Location

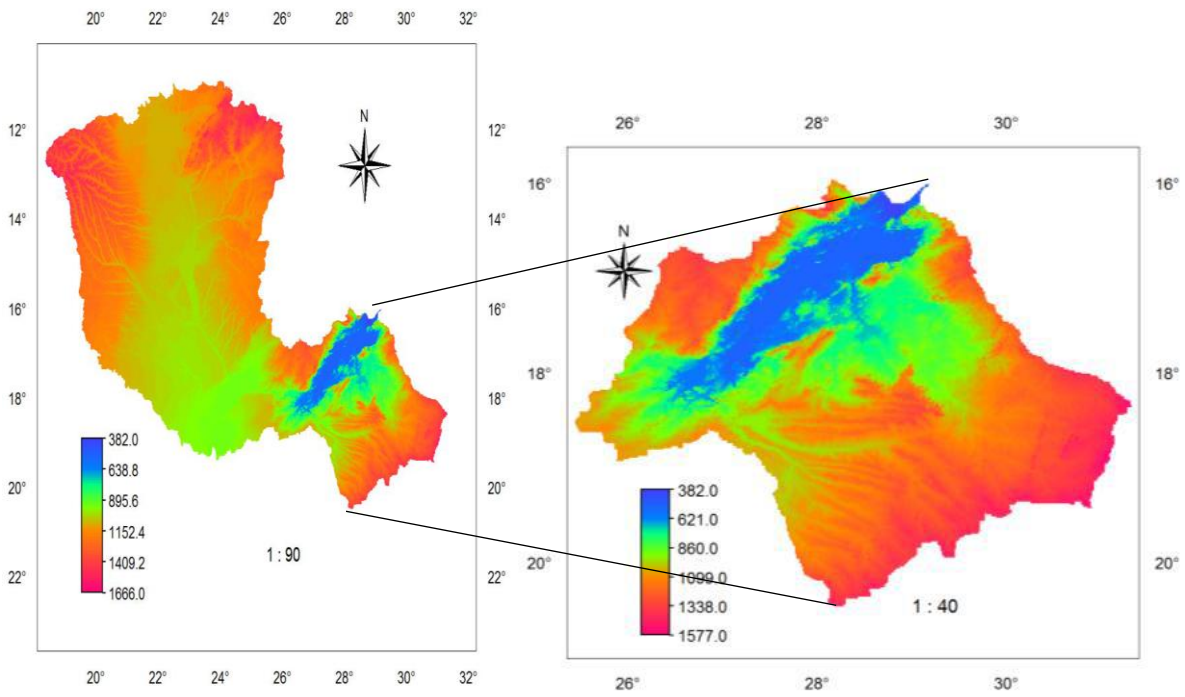

Figure 15. Digital elevation model of Kariba Catchment

3.2 Climate

According to Winsemius(2009), rainfall in the Zambezi River Basin is largely controlled by the Inter Tropical Convergence Zone (ITCZ) of which the Kariba Catchment lays. The ITCZ moves over the Zambezi basin from October to April, causing concentration of rainfall in the months of December to March. At the end of the dry season, the area receives least rainfall and mostly evaporation increases. Rainfall is usually high from December to February. July and August are the driest months with practically no rainfall received during these months.

3.3 Soils

There are seven types of soil in the catchment (Figure 16) which are classified under FAO (Food and Agriculture Organization) soil classification as Arenosols (18.4%), Cambisols (2.7%), Ferralsols (5.9%), Lithosols (21.7%), Luvisols (43.1%), Nitosols (3.5%) and Vertisols (0.9%) in combination with nine diagnostic horizon modifiers, namely, chromic, pellic, orthic, ferric, eutric, gleyic, cambic, luvic and vertic.

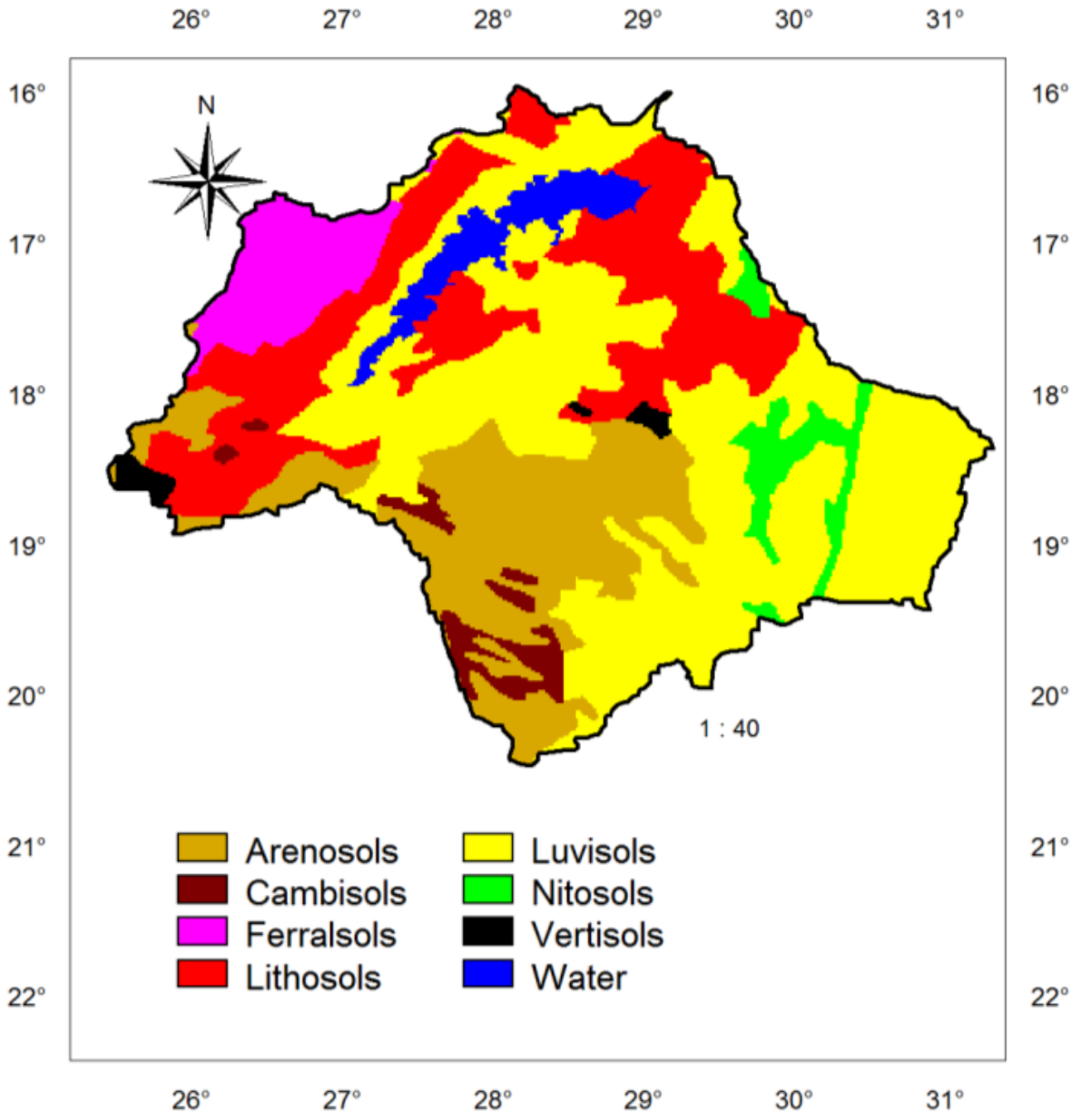

Figure 16. Kariba Lower Catchment major soil groups. Source (FAO, 2003)

3.4 Land cover

The land cover is dominated mainly by Rainfed agriculture (42.4%), Open woodland (36.8%), Grassland (8.3%), Evergreen forest (7%), Water (2.8%), Build-up (1.8%) and Deciduous forest (0.8%) as it is shown in Figure 17. Land cover data has been collected from ZRA and updated using global land classification.

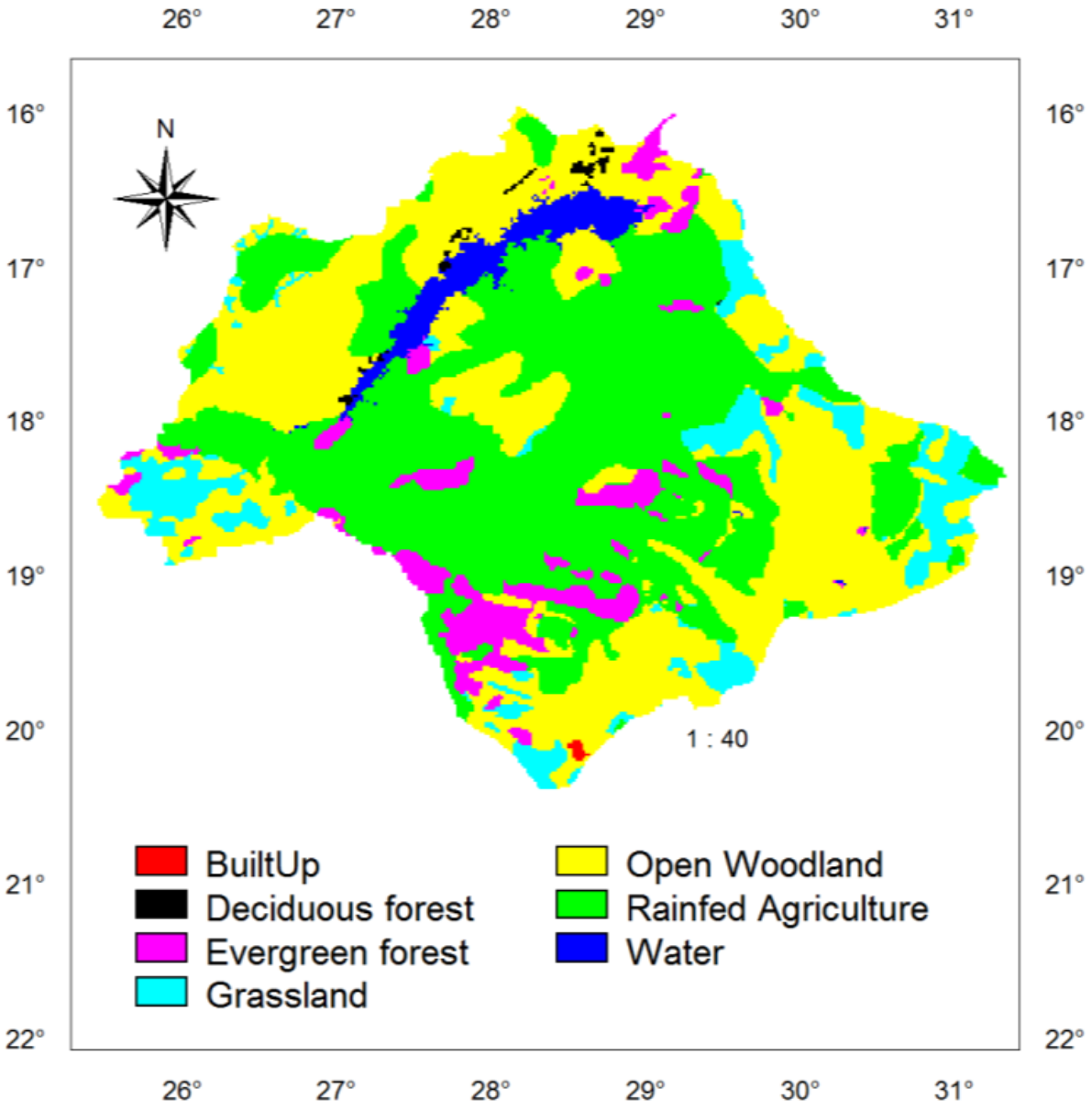

Figure 17. Land Cover of Kariba lower Catchment (Source. ZRA)

3.5 Drainage characteristics

Lake Kariba lower catchment is fed by flows from the upper and lower catchments. Flow from the upper catchment consists of Zambezi River (flow measured at Victoria Falls), whilst flow from the lower catchment consists of Gwayi, Sanyati, Sengwe, Kalomo, Ume and many small Rivers whose names are not known by the researcher, but used catchment numbering for the sake of this report), of which Gwayi, Sanyati are gauged. From January to June, Gwayi and Sanyati Rivers contribute an insignificant proportion of flows compared to flow measured at Victoria Falls.

CHAPTER 4: METHODOLOGY

Currently, there are a variety of methods used to quantify runoff in an ungauged catchment, all of which have their advantages and disadvantages. The approaches adopted for quantifying the runoff for the ungauged catchment of Lake Kariba lower are summarized in Figure 18.

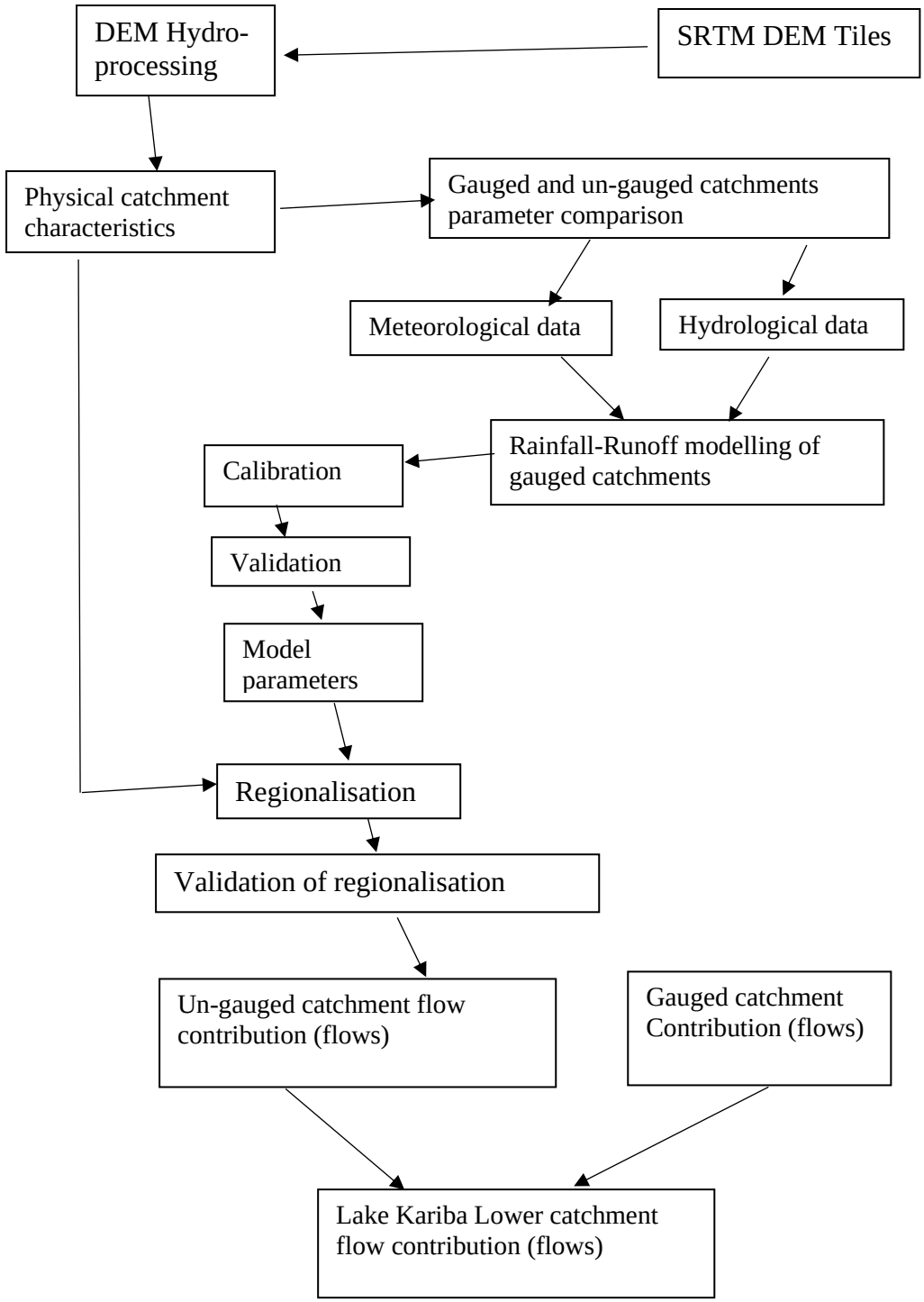

Figure 18. Methodology Adopted for the present Study

4.1 Data Availability

To simulate the runoff of Lake Kariba lower catchment, four types of data are used:

- Temperature and Precipitation data from National Aeronautics and Space Administration (NASA) Giovanni (Geospatial Interactive OnlineVisualization ANd aNalysis Infrastructure, https://giovanni.sci.gsfc.nasa.gov/) which is a Web based tool that allows users to access, visualize, and analyze vast amounts of Earth science remote sensing data without first having to download the data. The Web interfaces are designed to be clear and intuitive, facilitating data discovery, exploration and analysis of global and regional data sets covering atmospheric dynamics, atmospheric chemistry, hydrology, meteorology, precipitation, and oceanographic data. Giovanni portals provide an increasing amount of model output data in addition to the growing list of remote sensing data sets. Giovanni was developed by the Goddard Earth Sciences Data and Information Services Center (GES DISC).

- Flows for the gauged catchments of Sanyati and Gwayi to be used for the ungauged catchments model parameters estimation. This is achieved through by gleaning model parameters in ungauged catchments to the model parameters from hydrologically gauged similar catchments.

- Digital Elevation Model (DEM) from the Shuttle Radar Topography Mission (SRTM) which is a joint project of the National Imagery and Mapping Agency(NIMA) and the NASA to map the world in three dimensions. The SRTM instrument consisted of the Space borne Imaging Radar-C (SIR-C) hardware set modified with a Space Station-derived mast and additional antennae to form an interferometer with a 60-meter-long baseline. A description of the SRTM mission can be found in Farr & Kobrick (2000). The data for SRTM was downloaded from Earth Explorer (http://earthexplorer.usgs.gov), which provides online search, browse display, metadata export, and data download for earth science data from the archives of the U.S. Geological Survey (USGS). Earth explorer provides an enhanced user interface using state-of-the art JavaScript libraries, Hypertext Preprocessor (PHP), and the advanced Oracle spatial engine.

4.2 Data Processing

To achieve each specific objective, several methods are used to process the various data that was collected for it to be useful. The following sections illustrate in summary the methods used.

4.2.1 Temperature and Precipitation Data

The precipitation and temperature data was gotten from NASA Giovanni in a comma delimited text files for the period of 30th November 1998 to 31st March 2017 and 2nd January 2001 to 31st May 2017 for precipitation and temperature respectively. The spatial resolution of the precipitation data was 0.25º and temporal resolution of 1 day. Figure 19 and 20 show the precipitation and temperature time series area-averaged over the Lake Kariba Lower catchment respectively.

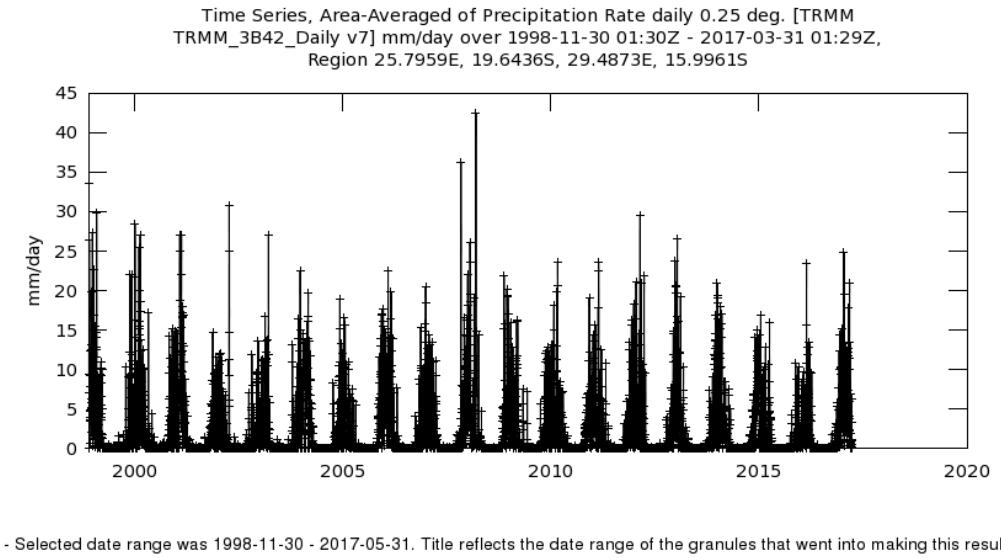

Figure 19. Lower Catchment Aerial Precipitation

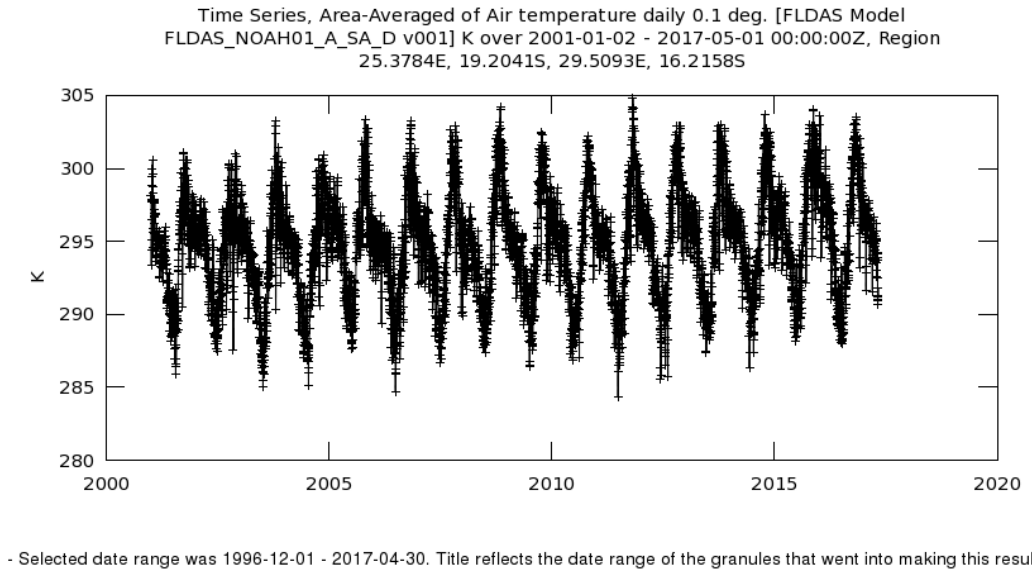

Figure 20. Lower Catchment Aerial Temperature

4.2.2 Gauged Catchment Flows

For this study, Sanyati and Gwayi Catchments were considered to be gauged catchments, with the rest of the lower Kariba catchments regarded as ungauged.

The Sanyati River is gauged at Binga Road Bridge (Yardley Bridge), and this site accounts for a large drainage area of inflows into the Lake after the Gwayi (SADC, 1994). It can be observed that the flows from Sanyati Catchment are of interest from December to May of each year, with the period January and March recording significant magnitude of flows as shown in Figure 21.

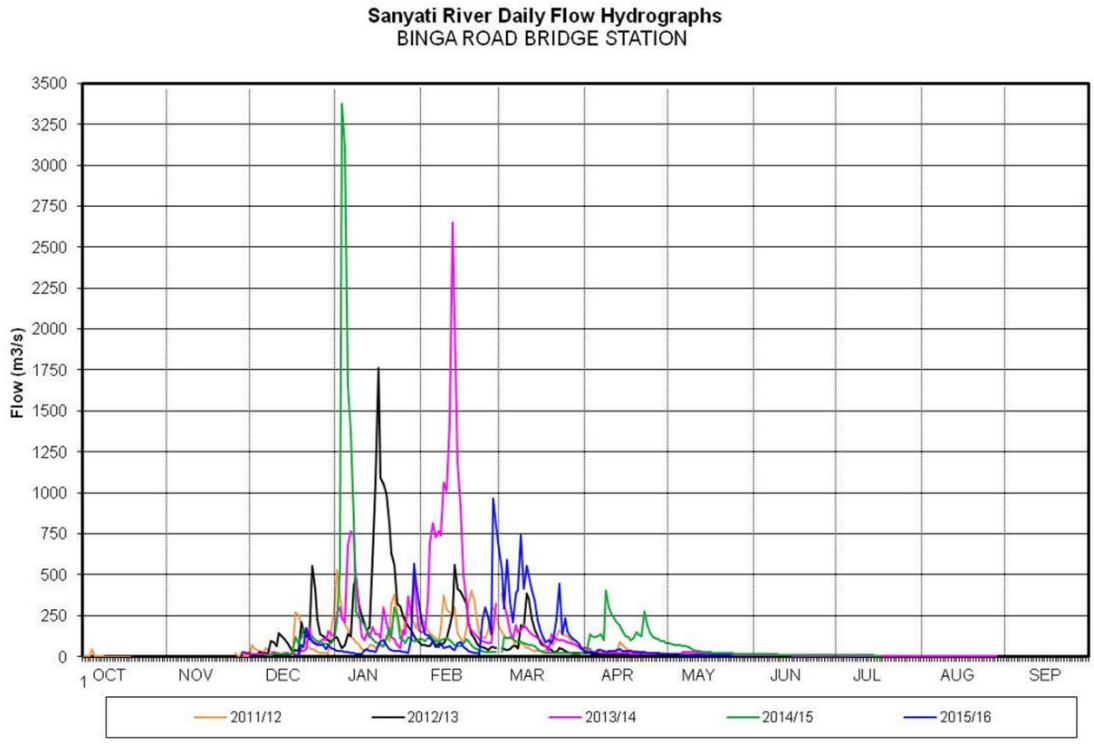

Figure 21. Sanyati River Daily flow hydrographs

The Gwayi river is the largest contributor of flows directly into the Lake Kariba from the lower catchment. The river is characterized by its flashy flows and also goes dry for several months each year like Sanyati river.

The analysis and use of hydrological data for decision making in water resources planning and management can only be meaningful if the data possess the appropriate characteristics. In general, it is customary that data being analyzed are consistent, free of trend and constituting a stochastic process whose random component is described by an appropriate probability distribution hypothesis. Consistency implies that all the collected data belong to the same statistical population. Trend exists in a data set if there is a significant correlation (positive or negative) between the observations and time. Trend or nonstationary is normally introduced through human activities such as land-use changes or the human induced climate change. In general, randomness in a hydrological time series means that the data arise from natural causes.

If there is no randomness, then the series is persistent (Adeloye & Montaseri, 2002). The stream flow data analyzed and selected was subjected to this evaluation, and that the record chosen was a continuous one.

4.2.3 Digital Elevation Model (DEM) Processing

In order to delineate the Lower Kariba catchment from a DEM in QGIS, the following steps were followed:

- Downloaded the DEM tiles of the study area, made sure that the tiles covered at least the study area and that the catchment of interest is covered completely. Its encouraged that one downloads larger tiles to avoid boundary effects.
- If a study area is covered by multiple DEM tiles, the tiles need to be mosaic (merge) to create a single raster DEM layer.
- The DEM tiles are usually in a different coordinate system than desired. The DEM was in its original Lat/Lon Geographic Coordinate System (EPSG: 4326). It was converted into the projection of the project. Because the project covers multiple countries, it will require not to use a local projection but a global projection: EPSG codes can be accessed at http://www.spatialreference.org. UTM Zone 35 South, with WGS-84 as datum and EPSG 32735 was used in the study area.
- The merged tiles were much larger than the study area, the tiles were subset (clip) into smaller area to reduce calculation time.
- Make a hydrological correct DEM by filling sinks and removing spikes from the raw DEM.
- Calculated the flow direction for each cell.
- Calculated the flow accumulation for each cell: how many upstream cells contribute to the runoff in each downstream cell of the DEM
- Derived the drainage network
- Calculated the catchment at the outflow point of the catchment

This flowchart below summarizes the procedure (Figure 22).

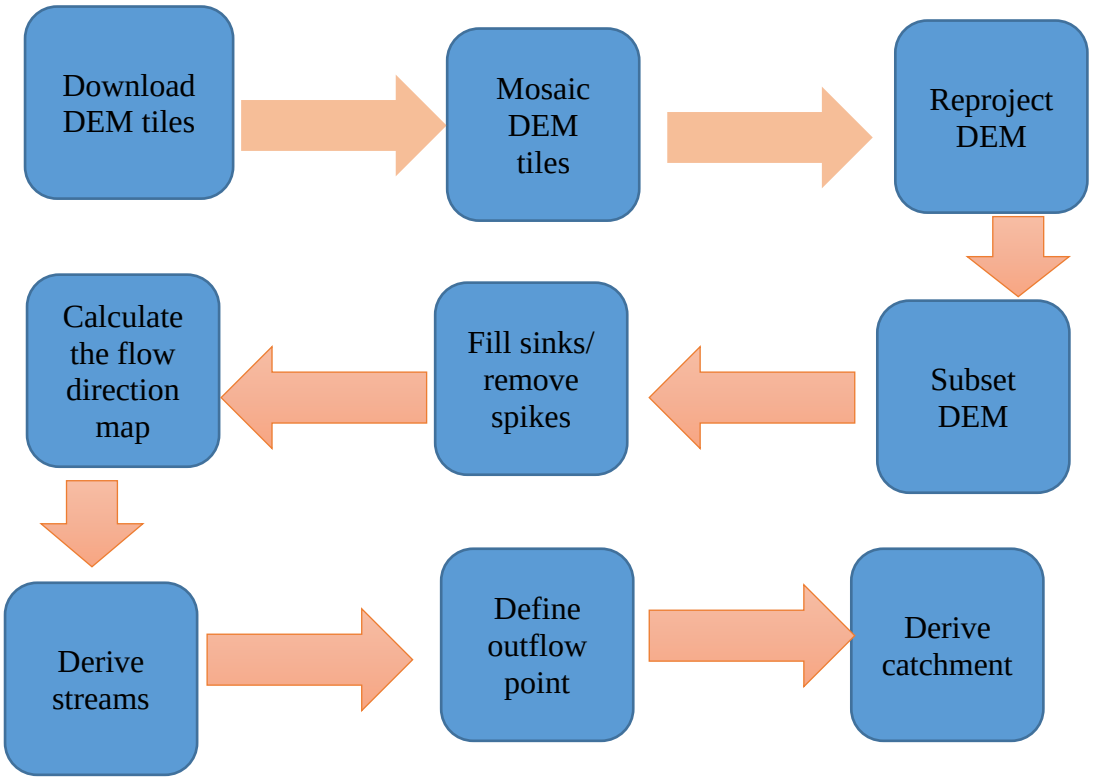

Figure 22 DEM Processing Flow chart

CHAPTER 5: RESULTS AND DISCUSSION

In this chapter, the findings of this study are presented, and the results are discussed with reference to other scientific works.

5.1 Results

This section presents results for the analysis for the input data into the RS Minerve such as flows from the two gauged hydro-met stations. It also presents comparisons between simulated flows and observed flows, with the other simulated flows for all the rest of the catchments are presented in the Appendix attached at the end of this report.

5.1.1 Lower Catchment model properties

The lower catchment was delineated into 12 sub-catchments as shown in Figure 23 and Table 4.

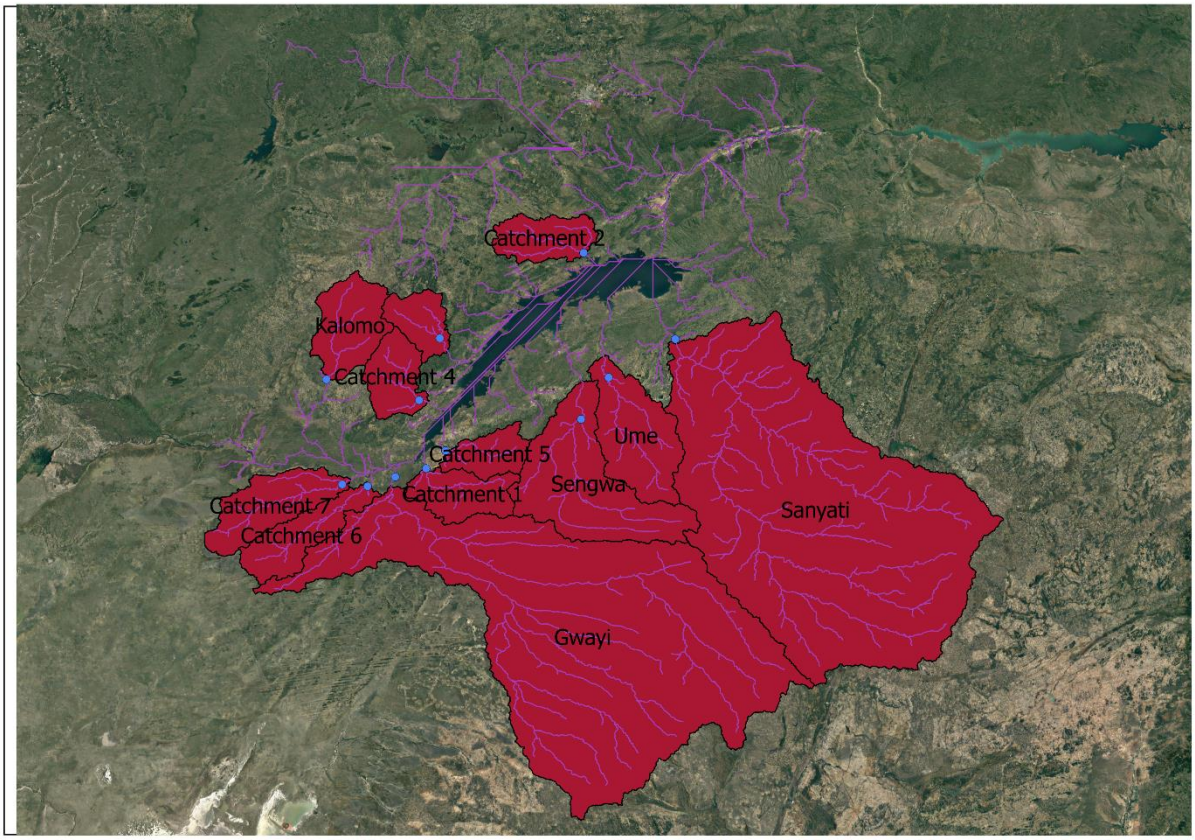

Figure 23. Sub Catchments of Lower Lake Kariba

Table 4. Sub Catchment of the Lake Kariba Lower Catchment

No.	Catchment Name	Area (Km^2)	Perimeter (Km)	Mean Slope
1	Catchment 1	2579	414	2.62
2	Catchment 2	2394	376	7.26
3	Catchment 3	1827	315	2.82
4	Catchment 4	2366	337	3.76
5	Catchment 5	1844	318	3.97
6	Catchment 6	3119	522	2.95
7	Catchment 7	3728	496	2.48
8	Gwayi	43082	2118	1.52
9	Kalomo	3414	419	1.35
10	Sanyati	42758	1574	2.09
11	Sengwa	8470	799	2.42
12	Ume	5156	544	2.74

The Gwayi Catchment is the Largest catchment in terms of area, seconded by Sanyati catchment. The lower catchment is characterized by steep slopes as shown in Table 4. Basic hydrological information such as, surface slopes, water flow paths positions, and soil and sub-basin distributions could easily be developed using QGIS. These datasets were later exported as text files or maps in shapefiles, TIFF, PNG or JEPG formats for presentation of results.

In this research, a database and hydrological model for the Lower Kariba catchment was successfully developed using remote sensing datasets, a GIS software QGIS and a rainfall-runoff software RS Minerve whose operating window is shown in Figure 24.

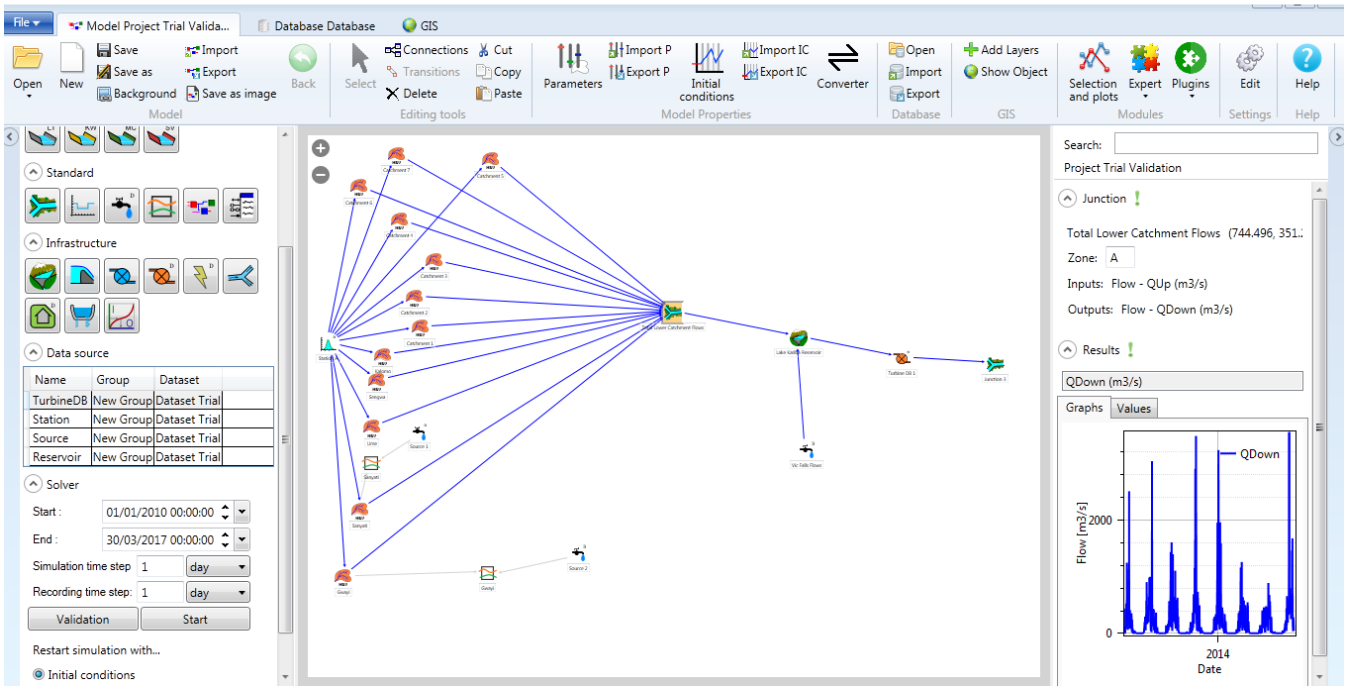

Figure 24. RS MINERVE Model of Lower Kariba Catchment

5.1.2 Gauged Catchment Flows

The Sanyati River is gauged at Binga Road Bridge (Yardley Bridge), and this site accounts for a large drainage area of inflows into the Lake seconded by Gwayi (SADC, 1994). It can be observed that the flows from Sanyati Catchment are of interest from December to May of each year, with the period January and March recording significant magnitude of flows. The Gwayi river is the largest contributor of flows directly into the Lake Kariba from the lower catchment. The river is characterized by its flashy flows and also goes dry for several months each year like Sanyati river.

For the sake of this study flows from 01 July 2002 to 31 July 2007 were used to derive the catchment parameters that were further transferred to other sub-catchments as they have been considered to behave in a similar manner hydrologically based on the principles of regionalisation. The chosen dataset was used to compare with the simulated flows for the two gauged catchments as shown in the Figures 25 and 26.

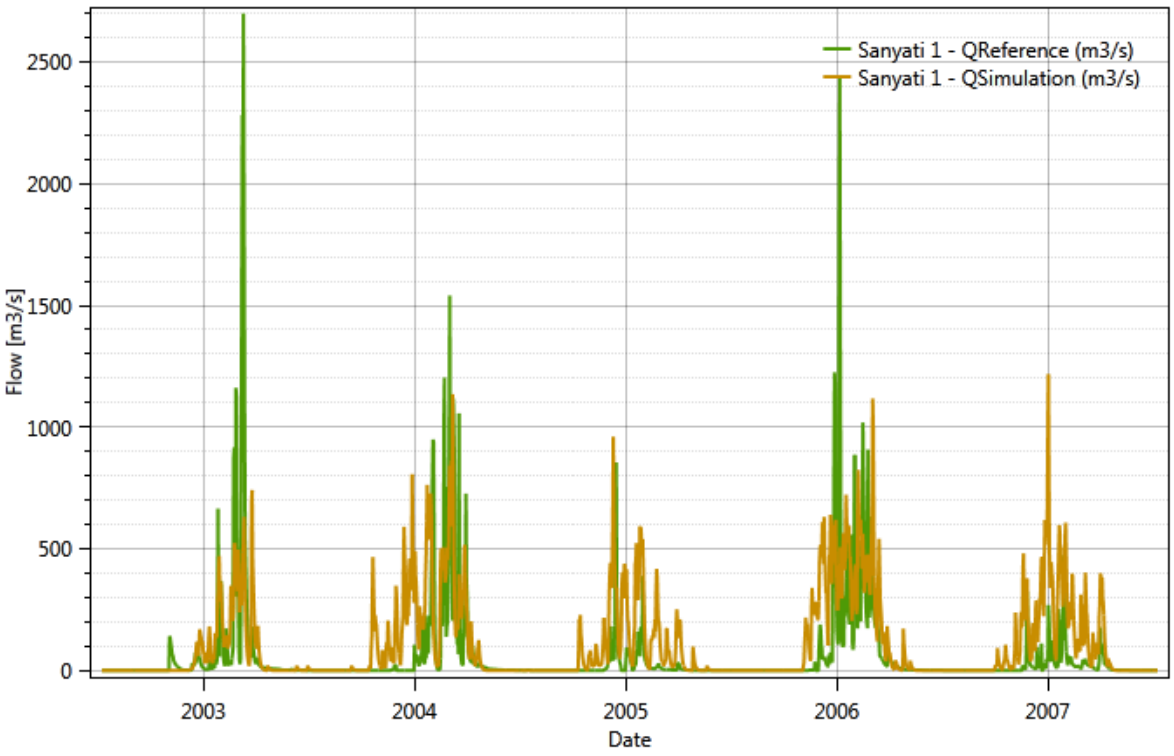

Figure 25. Model performance for Sanyati Catchment

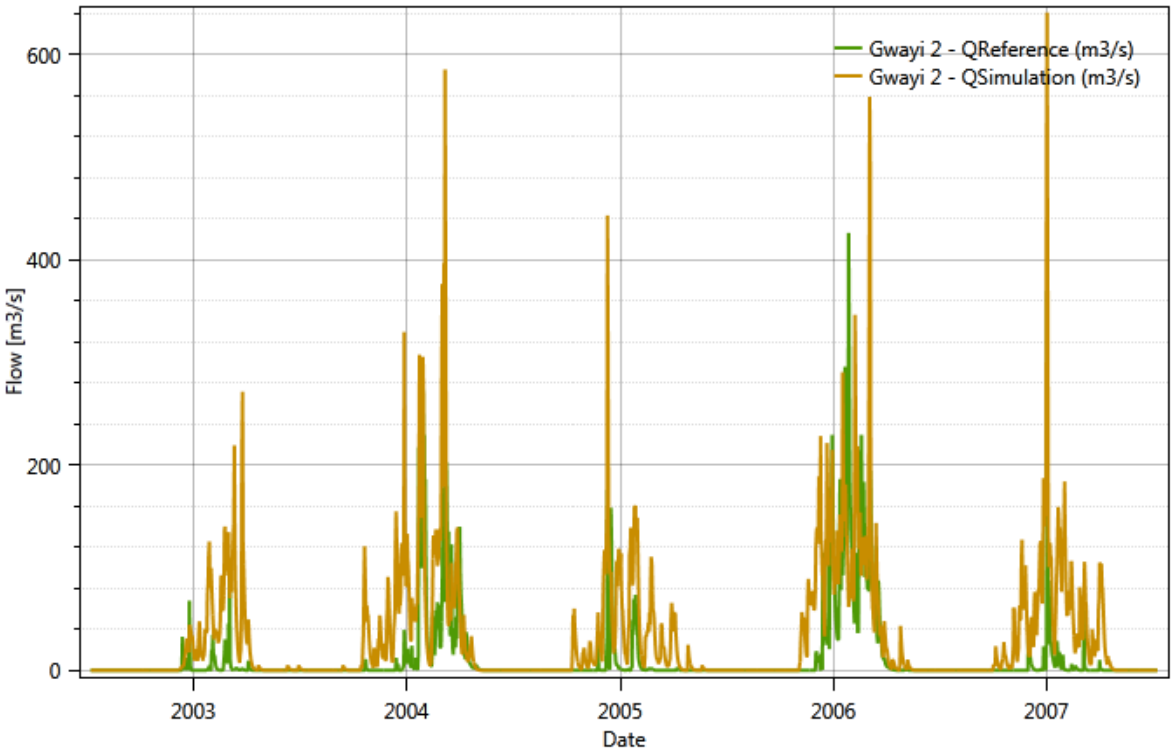

Figure 26. Model performance for Gwayi Catchment

The performance of the model can be explained based on the recommended ranges of indicators: If the Nash-Sutcliffe coefficient (NSC) which is used to assess the predictive power of hydrological models has values greater than 0.75 are considered to show good model efficiency, Nash of between 0.36 and 0.75 shows satisfactory performance and values less than 0.36 are considered to be unsatisfactory (Motovilov, et al., 1999). Table 5 shows the model performance indicators when the model was run on a daily time step.

Table 5. Model performance indicators at daily time step

	SANYATI MODEL INDICATORS	GWAYI MODEL INDICATORS	RANGE OF VALUES	IDEAL VALUE
NASH	0.15	-0.57	-∞ to 1	1
NASH-in	0.63	0.67	-∞ to 1	1
PEARSON CORRELATION	0.48	0.43		1
KLING-GUPTA EFFICIENCY	0.17	0.07	-∞ to 1	1
BIAS SCORE	0.81	0.91	0 to 1	1
RRMSE	3.10	4.10	0 to +∞	0
RELATIVE VOLUME BIAS	0.43	-0.24	-∞ to +∞	0
NORMALIZED PEAK ERROR	-0.52	0.97	-∞ to +∞	0

It can be noted that the performance of the model at daily time step was generally poor as shown in Table 5. Table 6 shows the model performance indicators for the same two gauged stations for a monthly time step and it can be noted further that the model performed very well at monthly time step.

Figure 27 and 28 shows the performance of the model for the two gauged catchments of Sanyati and Gwayi with both showing satisfactory indicators as shown in Table 6, except for the KGE which showed slightly lower value on variability ratio, i.e., ratio between the coefficient of variation of the simulated values and the coefficient of variation of the reference one on the Sanyati Model than the Gwayi.

The Sanyati and Gwayi flows were validated for the period 1 October 2007 to 30 September 2008. The results obtained showed good model efficiency as shown in Figures 27 and 28 with the corresponding model indicators given in Table 6.

Table 6. Model performance indicators at monthly time step

	SANYATI MODEL INDICATORS	GWAYI MODEL INDICATORS	RANGE OF VALUES	IDEAL VALUE
NASH	0.52	0.54	-∞ to 1	1
NASH-IN	0.68	0.75	-∞ to 1	1
PEARSON CORRELATION	0.77	0.76		1
KLING-GUPTA EFFICIENCY (KGE)	0.41	0.61	-∞ to 1	1
BIAS SCORE	0.82	0.90	0 to 1	1
RRMSE	1.45	1.68	0 to +∞	0
RELATIVE VOLUME BIAS	0.42	-0.24	-∞ to +∞	0
NORMALIZED PEAK ERROR	-0.29	-0.39	-∞ to +∞	0

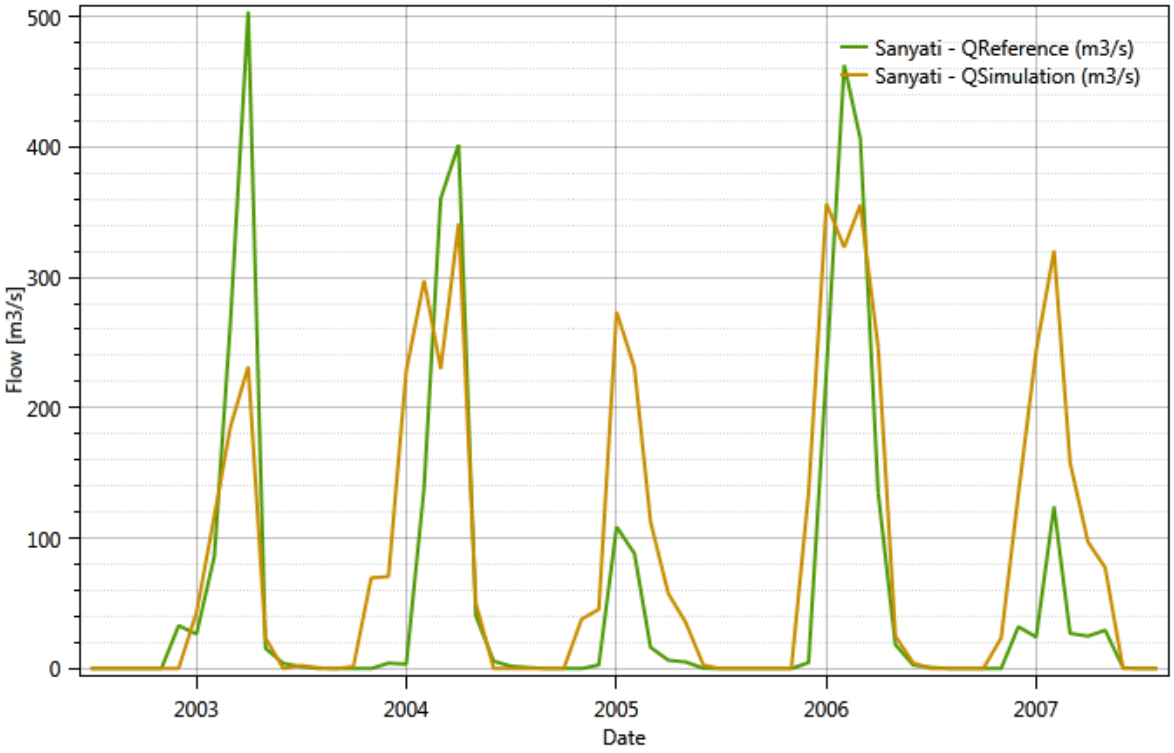

Figure 27. Sanyati model performance at monthly time step

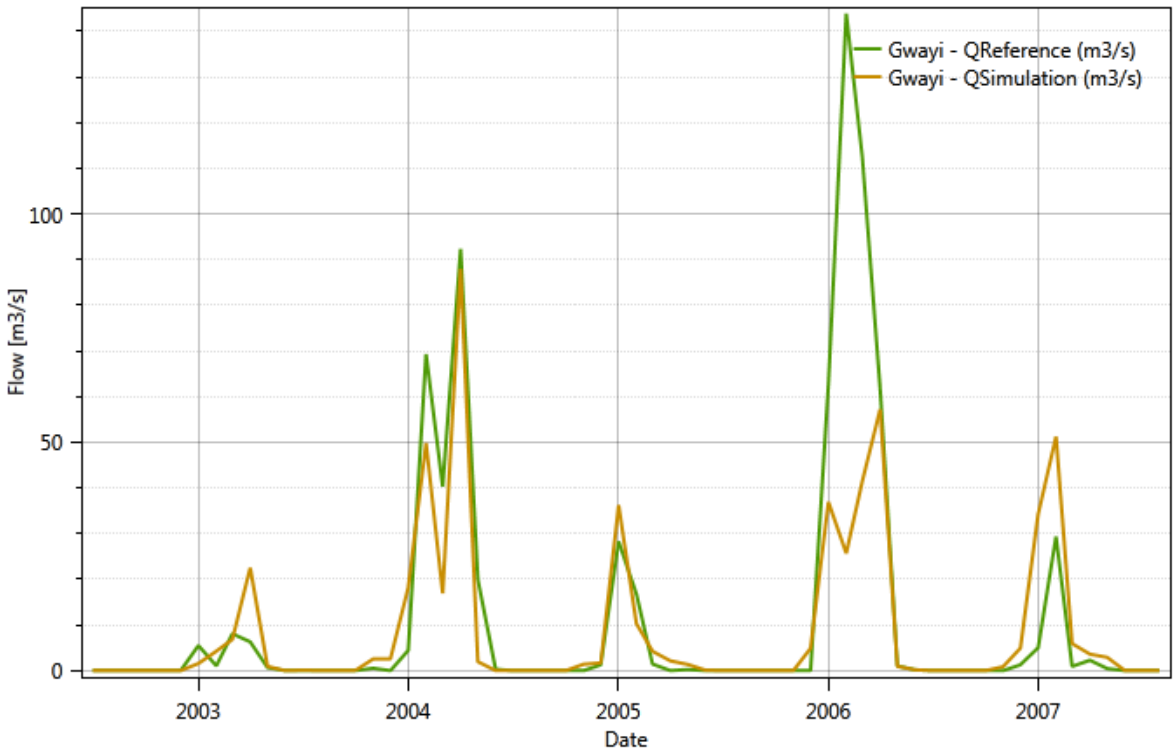

Figure 28. Gwayi model performance at monthly time step

5.1.3 Ungauged catchments flow

Regionalization was then conducted on all ungauged catchments by transferring of model parameters from the gauged catchments to the ungauged catchments and the results are shown in the hydrographs in the Appendix.

5.1.4 Lower Catchment flows

The sub-catchment contributions were amalgamated to a single contribution into Lake Kariba as shown in Figure 29 for the simulated lower catchment flows for the period 01 January 2010 to 30th March 2017 and figure 30 showing the comparison plot of Lower catchment flows to Vic Falls flows. Table 7 shows comparison of yearly Lower Kariba Catchment to that of Victoria Falls Gauging Station.

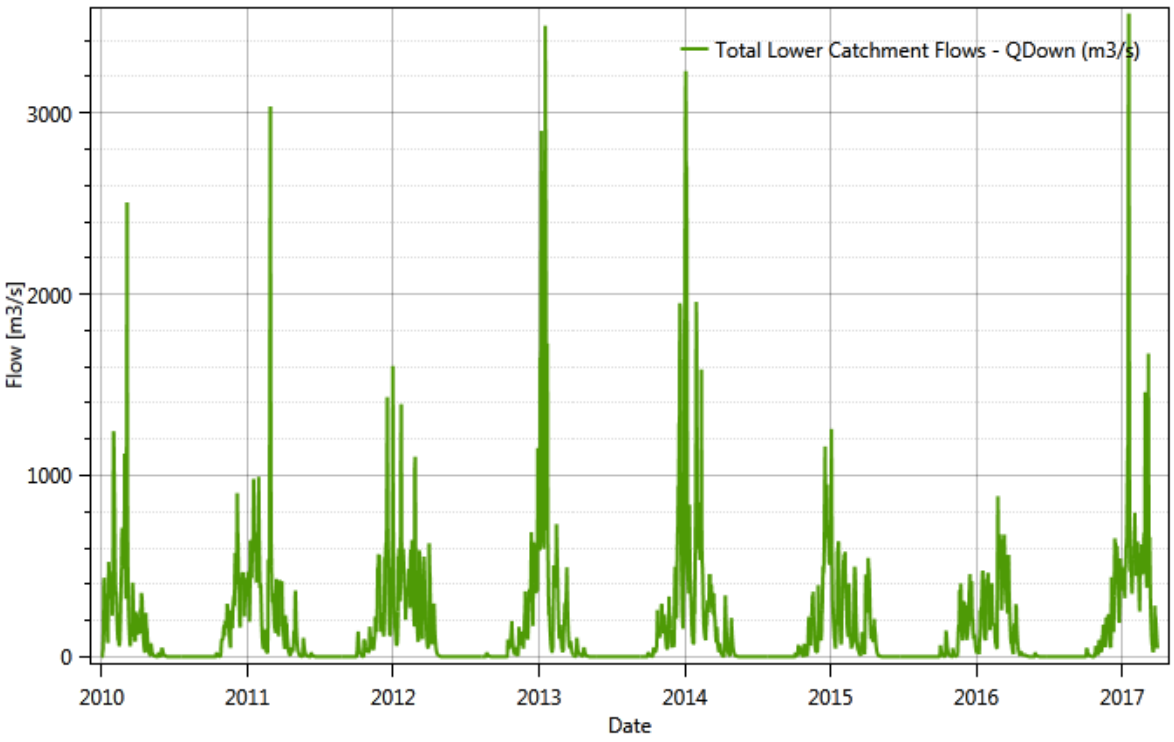

Figure 29 Total inflow from the lower sub catchments

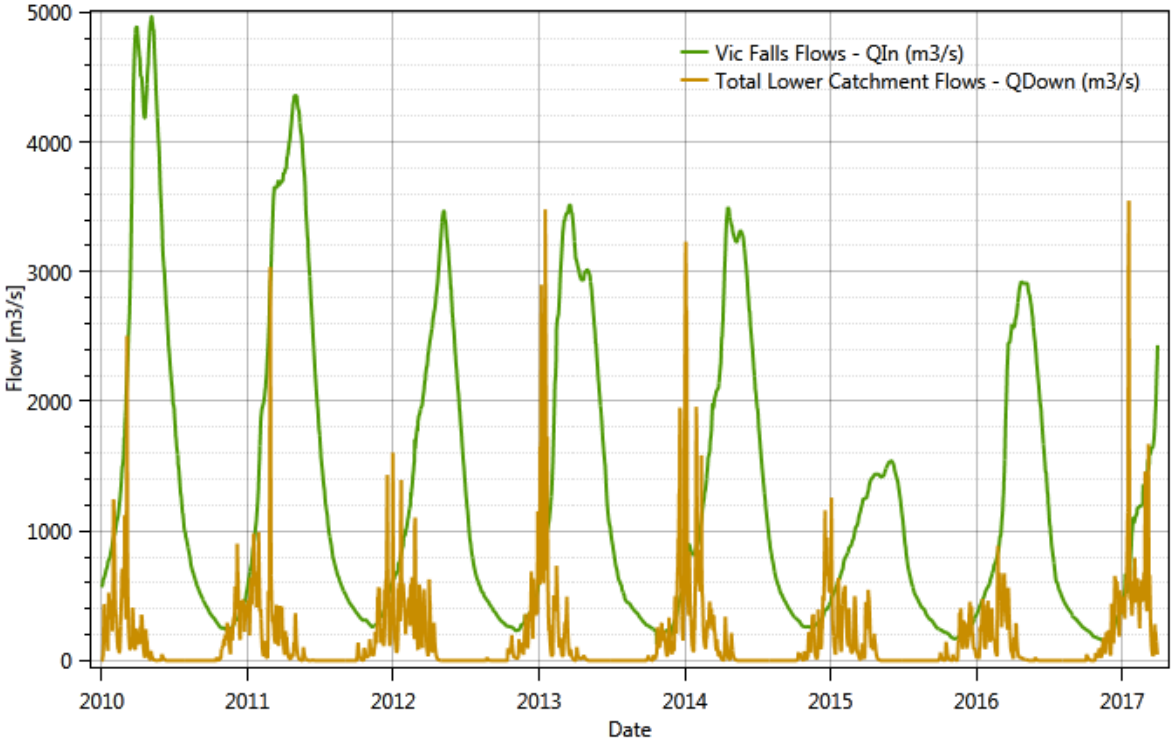

Figure 30 Victoria falls flows vs lower catchment flows

Table 7 Comparison of lower Kariba and Victoria Yearly Flows

YEAR	LCF/YEAR (M^3/S)	VCF/YEAR (M^3/S)	% DIFF
2010	57,849.09	622,356.88	9
2011	62,612.90	624,246.87	10
2012	54,796.72	449,201.03	12
2013	69,628.25	489,275.18	14
2014	69,961.61	496,403.31	24
2015	38,879.76	270,333.36	14
2016	43, 282.32	378,258.85	11
2017*	49,850.91	107,105.76	47

*It should be noted that for the year 2017, its from 1st January 2017 to 30th March 2017

5.2 Discussion

5.2.1 Model Performance, uncertainties and solutions

The model was successfully calibrated and validated with flows for Sanyati and Gwayi and its performance was evaluated based on the two gauging stations. The comparison between the observed and simulated stream flow indicated that there was a good agreement between the observed and simulated discharge of the calibrated model at monthly time step which was evidenced by higher values of Pearson coefficient, Bias Score (BS), Nash-Sutcliff efficiency (NSE) and fairly good agreement in the hydrographs. The model evaluation statistics for stream flows gave acceptable results that ranged from satisfactory to good. The poor model performance at daily time step could be due to poor quality of the gauged climate variables as well as the very coarse spatial distribution of weather stations in the sub-watersheds. Even though the model performed in a satisfactory level, the performance level should not be generalized equally for all purposes. As introduced in Razavi & Coulibaly (2012), regionalization is more efficient for warm temperate regions. (Razavi & Coulibaly, 2012), hence the adoption of this methodology.

Although ASCE (1993) emphasized the need to clearly define model evaluation criteria, no commonly accepted guidance has been established, but specific statistics and performance ratings for their use have been developed and used for model evaluation (Motovilov, et al., 1999). However, no comprehensive guidance is available to facilitate model evaluation in terms of the accuracy of simulated data compared to measured flow and constituent values. Jiyun, et al. (2016) recommended that three quantitative statistics, Nash-Sutcliffe efficiency (NSE), percent bias (PBIAS), and ratio of the root mean square error to the standard deviation of measured data (RSR), in addition to the graphical techniques, be used in model evaluation. The following model evaluation performance ratings were established for each recommended statistic. In general, model simulation can be judged as satisfactory if NSE > 0.50 and RSR < 0.70, and if PBIAS 25% for streamflow. In comparison with the finding of this study, it can be established that the model performed well as shown by the validated indicators in Table 8 and corresponding validated hydrographs in Figure 31 and 32. It is worth noting that the PBIAS

is referred to as Relative Volume Bias (RVB), sometimes called differently (Ajami, et al., 2004, AghaKouchak & Habib, 2010,and Moriasi, et al., 2007).

In general, flow dynamics of a catchment is closely related to dominant climatic conditions and catchment characteristics (Jiyun, et al., 2016), in the lower Kariba catchment, the selected catchments have assumed similar climatic conditions. Hence the differences caused by the underlying surface characteristics, including soil moisture, soil properties, soil structure, vegetation conditions, topography and many others have been ignored in this research. Which could have led to getting unsatisfactory results at daily time step. It's worth noting that Jiyun, et al (2016) considered these factors when a study was conducted on how to predict streamflow in ungauged catchment in Huai basin in china, it was found that it improved the results of the predicted flows at daily time step.

Table 8 Model Validation Indicators

	SANYATI MODEL INDICATORS	GWAYI MODEL INDICATORS	RANGE OF VALUES	IDEAL VALUE
NASH	0.71	0.75	-∞ to 1	1
NASH-IN	0.82	0.64	-∞ to 1	1
PEARSON CORRELATION	0.89	0.87		1
KLING-GUPTA EFFICIENCY (KGE)	0.69	0.83	-∞ to 1	1
BIAS SCORE	0.94	0.98	0 to 1	1
RRMSE	1.08	1.10	0 to +∞	0
RELATIVE VOLUME BIAS	-0.19	-0.11	-∞ to +∞	0
NORMALIZED PEAK ERROR	-0.37	-0.05	-∞ to +∞	0

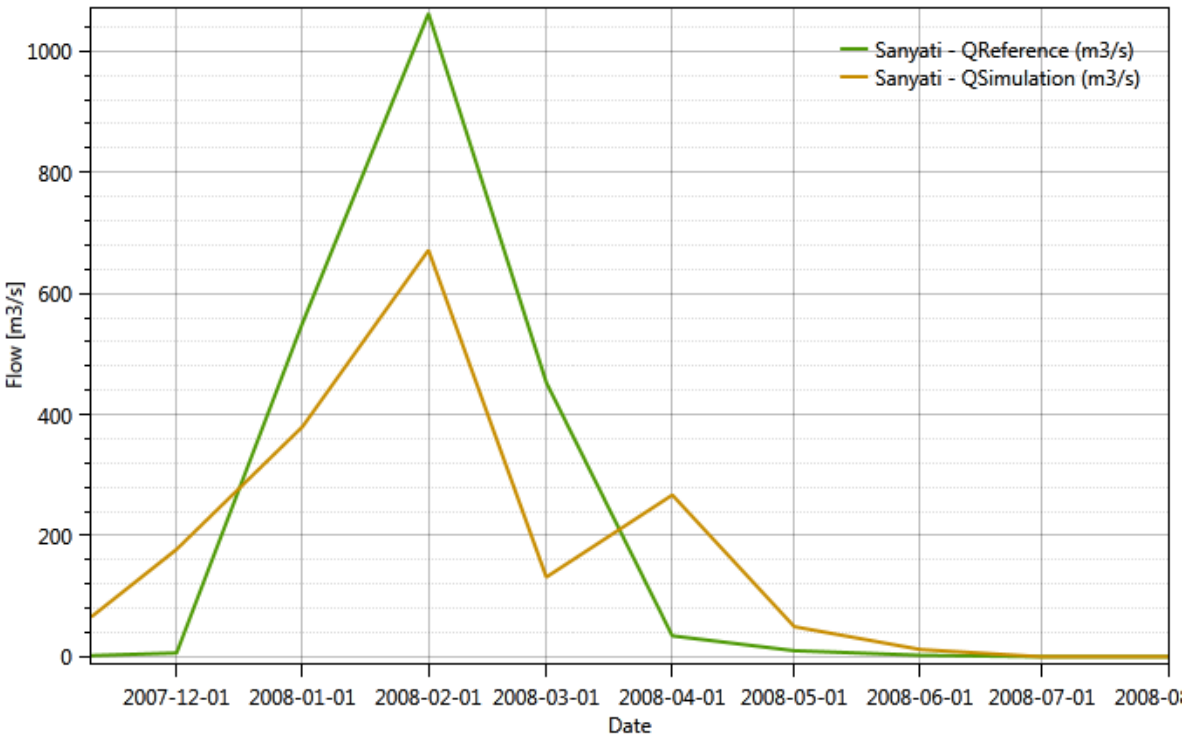

Figure 31 Sanyati validation hydrograph

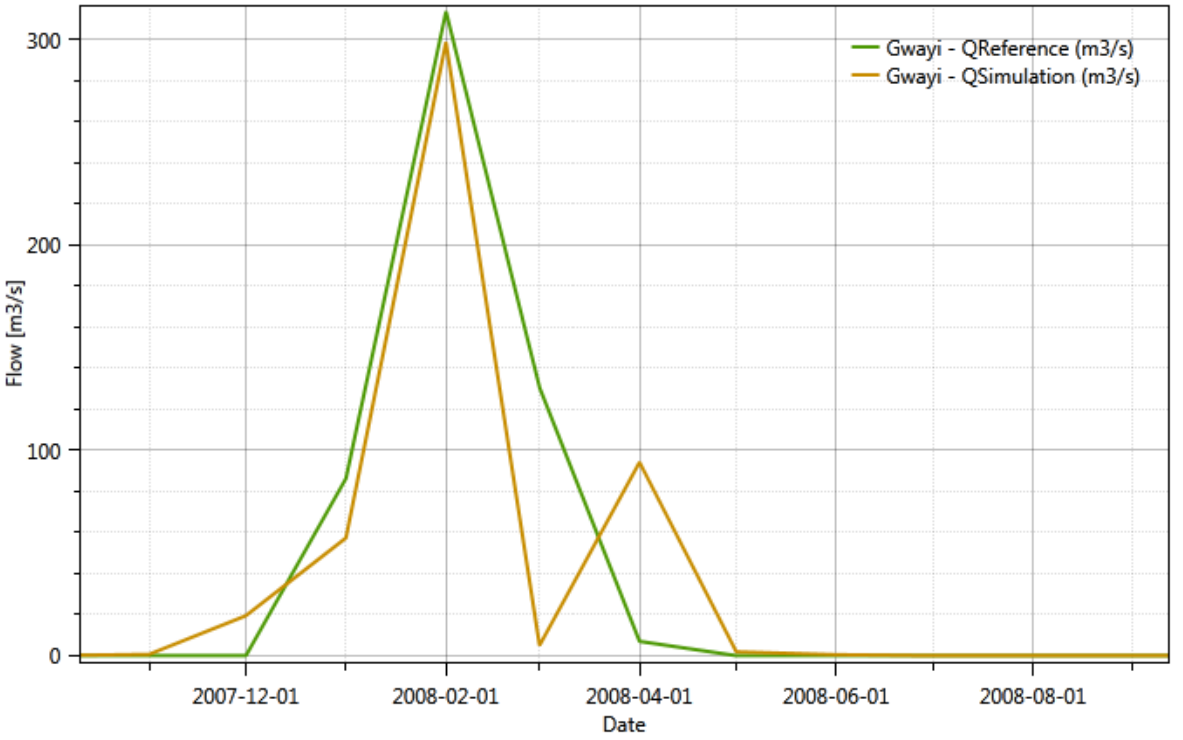

Figure 32 Gwayi validation hydrographs

It is noteworthy that the selected study area is subject to human interference such as the presence of small irrigation dams, the original hydrographs having been changed over the course of the years. The reconstruction of natural streamflow presents a challenge due to the lack of operation data of these small dams, especially for high flows when they are discharging.

5.2.2 Possible applications for the developed hydrological model

The study showed that the monthly flows were better simulated than the daily flows. It should be noted that the daily results are much more important than the monthly if the simulation is for flood analyses and flood protection or prevention plans. By contrast, for hydropower and irrigation purposes the monthly results could be used for allocating and planning water resource. Since the primary application of the RS MINERVE model is for land management and agriculture, the calibrated model can be used to analyze the effects of change in land use and different management scenarios on stream flow regimes. The evaluation of the model indicate that care must be taken on direct transferring of parameter values in association to watershed characteristics, with emphasis on drainage area.

The model can be further used for reservoir operations, the design of drainage structure and flood defenses in these ungauged catchments, runoff forecasting. More importantly the growing populations, contaminated supplies, and potentially changing supplies, have come under much more scrutiny in the recent years. The amount of water crossing political boundaries as is the case of Lake Kariba lower catchment were water is mostly generated from Zambia and Zimbabwe, and issues of equal and equity contributions of water are constantly being raised in the political corridors.

.

CHAPTER 6: CONCLUSIONS AND RECOMMENDATIONS

One of the main objectives of this study is to simulate runoff for the Ungauged sub-catchments of Lake Kariba lower catchment. Rainfall-runoff modelling for ungauged catchment is data driven. The various dataset required were obtained and processed such as satellite meteorological observations like precipitation and temperature, images and DEM for Kariba Lower Catchment. The river flow from un-gauged catchments is simulated by transferring model parameters of gauged catchments through regionalisation. This approach converts rainfall to streamflow through physically based mathematical transformations without information of evaporation or soil moisture. The model can be further improved with more available measurement datasets as well as regional geographic information for example, anthropogenic factors will be critical in understanding the evolution of catchments' hydrological responses to potential landscape modification scenarios.

6.1 Conclusions

Based on the study conducted, the following conclusions are drawn:

i. Rainfall and Temperature dataset from remote sensing can be adequately used to simulate runoff in the ungauged Lake Kariba Catchment.

ii. The average runoff of the lower Kariba catchments is about 12% of the total yearly runoff recorded at Victoria falls gauging station.

iii. The rating equations for Sanyati and Gwayi Rivers have been the same since their development while their channels are ever changing due to the nature of the flow regime.

6.2 Recommendations

To further enhance the results of the Lake Kariba Lower catchment runoff; the following recommendations are formulated:

i. Research has to be conducted on how to improve Daily runoff simulations for flash rivers of the Lower Kariba catchment.

ii. More Rating equation updating, and validation missions should be undertaken to ascertain the validity of discharge stage relationship as these are flash rivers whose channel is ever changing every year.

iii. Gauging more of the un-gauged catchments and further studies should be conducted regarding Lake evaporation, rainfall on the Lake and Turbine flow measurements in order to help validate the Lower Catchment flows with the inflow in the Lake.

REFERENCES

(IH), I. o. H., 1999. *Flood Estimation Handbook.* UK: Wallingford.

Abbott, M. B. et al., 1986b. An introduction to European Hydrological System (SHE). Part 2. Structure of a physically based distributed modeling system. *Journal of Hydrology,* Issue 87, pp. 61-77.

Adeloye, A. J. & Montaseri, M., 2002. Preliminary Streamflow data analysis prior to water resources planning study. *Hydrological Sciences,* 45(5), pp. 679-692.

AghaKouchak, A. & Habib, E., 2010. Application of a conceptual Hydrologic model in Teaching Hydrologic Processes. *International Journal of Engineering Education,* 4(26), pp. 963-973.

Ajami, N., Gupta, H., Wagener, T. & Sorooshian, S., 2004. Calibration of semi-distributed hydrologic model for streamflow estimation along a river system. *Journal of Hydrology,* Issue 298, pp. 112-135.

Archfield, S. A. & Vogel, R. M., 2010. Map correlation method: Selection of a reference Streamgauge to estimate daily streamflow at ungauged catchments. *Water Resources Research,* Issue 10, p. 46.

ASCE, 1993. Criteria for Evaluation of watershed Models. *Irrigation Drainage Engineering,* 3(119), pp. 429-442.

Batoka Joint Venture, C., 1993. *Batoka Gorge Hydro Electric Scheme - Feasibility Report,* Lusaka: Batoka Joint Venture Consultants.

Bergstrom, S., 1976. *Development and application of a conceptual runoff model for Scandinavian catchments. Ph.D Thesis,* s.l.: s.n.

Bergstrom, S., 1992. *The HBV model- Its structure and applications,* Norrkoping: s.n.

Beven, K., 2012. *Rainfall-Runoff Modelling. The Primer.* 2 ed. Lancaster University, UK: John Wiley & Sons.

Bloschl, G., 2005. Rainfall-Runoff of ungauged catchments. In: M. G. Anderson, ed. *Encyclopaedia of hydrological Sciences.* UK: John Wiley & Sons, pp. 2061-2080.

Bloschl, G. & Sivapalan, M., 1995. Scale issues in Hydrological Modelling. *Hydro Processes,* Issue 9, pp. 251-290.

Brutsaert, W. & Mawdsley, J. A., 1971. The application of planetarylayer theory to calculate regional evaporation. *Water Resource,* Issue 12, pp. 852-858.

Chow, V., Maidment, D. & Larry, W., 1988. *Applied Hydrology.* s.l.:McGraw.

Dooge, J. C., 1972. *Mathematical models of hydrologic systems. Proceedings of the International Symposium on Modelling Techniques in Water Resources Systems.* Ottawa, s.n.

Duan, Q., Sorooshian, S. & Gupta, V., 1994. Optimal use of SCE-UA global optimisation method for calibrating watershed models. *Journal of Hydrology,* Volume 158, pp. 265-284.

Elachi, C. & Zyl, V., 2006. *Introduction to the physics and techniques of remote sensing.* s.l.:John Wiley & Sons.

FAO, 2003. *The digital soil map of the world,* Rome, Italy: s.n.

Farr, T. G. & Kobrick, M., 2000. Shuttle Radar Topography Mission produces a wealth of data. *American Geophysics ,* Volume 81, pp. 583-585.

Federal Power Board, 1959. *Report on the Requirements for Further Hydrological Studies of the Zambezi River Upstream of Kariba,* Rhodesia and Nyasaland: Federal Power Board.

Feyen, L. et al., 2000. Application of a physically based distributed hydrological model to a medium size catchment. *Hydrology and Earth sciences,* 1(4), pp. 47-63.

Freeze, R. A., 1971. Three-dimensional, trnasent, saturated-unsaturated flow in a groundwater basin. *Water Resources,* 2(7), pp. 347-366.

Gabellani, S. et al., 2007. Propagation of Uncertainty from rainfall to runoff. A case study with a stochastic rainfall generator. *Advances in Water Resources,* Volume 30, pp. 2061-2071.

Gayathri, D. K., Ganasri, B. P. & Dwarakishi, G. S., 2015. *A Review of Hydrological Models.* s.l., International Conference on Water Resources, Coastal and Ocernic Engineering.

Gupta, H., Kling, H., Yilmaz, K. & Martinez, G., 2009. Decomposition of the mean squared error and NSE performance criteria: Implications for improvinghydrological modelling. *Journal of Hydrology,* Volume 377, pp. 80-91.

Hernandez, G. J., 2011. *Flood management in a complex river basin with real time decision support system based on the hydrological forecasts: PhD Thesis,* Switzerland: s.n.

Hernandez, G. et al., 2017. *Technical Manual v 2.9 RS MINERVE,* Switzerland: RS MINERVE GROUP.

Jeremiah, E., Sisson, S., Sharma, A. & Marshall, L., 2012. Efficient hydrological model parameter optimisation with sequential Monte carlo sampling. *Environmental modelling and software,* Volume 38, pp. 283-295.

Jiyun, S. et al., 2016. Streamflow prediction in ungauged basins by regressive regionalisation: A case study in Huai River Basin, China. *Hydrology Research,* 5(45), pp. 1053-1068.

Kamali, M., Ponnambalam, K. & Soulis, E. D., 2013. Comparisons of several heuristic approaches to calibration of WATCLASS hydrologic model. *Canadian Water Resources,* 38(1), pp. 40-46.

Kang, F., Li, J. & Ma, Z., 2011. Rosenbrock artificial bee colony algorithm for accurate global optimization of numerical functions. *Information sciences,* 181(16), pp. 3508-3531.

Kirby, M., 1978. *Hillslope Hydrology. Landscape systems, a series in geomorphology.* UK: John Wiley and sons.

Kling, H., Fuchs, M. & Paulin, M., 2012. Runoff conditions in the upper Danube basin under an ensemble of climate change scenarios. *Journal of Hydrology,* Volume 424-425, pp. 264-277.

Lenhart, K. T., Eckhardt, N., Fohrer, N. & Frede, H. G., 2002. Comparison of two different approaches of sensistivity analysis. *Physics and Chemistry of the Earth,* pp. 645 -654.

Lillesand, T. M., Kiefer, W. & Chipman, W., 2004. *Remote sensing and image interpretation.* 5 ed. New York: John Wiley & Sons.

Liu, J. S., 2001. *Monte Carlo Strategies in Scientific Computing.* New York: Springer Verlag.

McKay, M. D., Beckman, R. J. & Conover, W., 1979. A comparison of three methods for selecting values of input variables in the analysis of output from a computer code. *Technometrics,* 21(2), pp. 239-245.

Merz, R. & Bloschl, G., 2004. Regionalisation of catchment model parameters. *Journal of Hydrology,* 1(4), pp. 95-123.

Merz, R., Bloschl, G. & Parajka, J., 2006. Regionalisation methods in rainfall-runoff modelling using large catchment samples. *Journal of Hydrology,* pp. 117-125.

Metcalf & Eddy, 1971. *Storm Water management model. Vol 1, Final Report,* Washington: EPA.

Moradkhani, H. & Sorooshian, S., 2008. General review of rainfall-rainfall modelling: model calibration, data assimilation and uncertainty. *Hydrological modeling and water cycle,* Issue 4, p. 291.

Morel-Seytoux, H. J., 1978. Derivation of equations for variable rainfall infiltration. *Water Resources,* 4(14), pp. 561-568.

Moriasi, D. et al., 2007. Model evaluation guidelines for systematic quantification of accurancy in watershed simulations. *American Society of Agricultural and Biological Engineers,* 3(50), pp. 885-900.

Moriasi, D. N. et al., 2007. Model Evaluation Guidlines for Systematic Quantification of Accurancy in Watershed Simulations. *American Society of Agricultural and Biological Engineers (ASABE),* 50(3), pp. 885-900.

Motovilov, Y. G., Gottschalk, L., Engeland, K. & Rodhe, A., 1999. Validation of a distributed hydrological model against spatial observations. *Agricultural and forest Meteorology,* 99(98), pp. 257-277.

Muzumara, M., 2011. *Application of Remote Sensing Using a GIS Based Soil Water assessment Tool (SWAT) to Estimate River Discharge in the Kabompo River Basin, Zambia,* Lusaka, Zambia: Unpublished MSc, School of Mines, University of Zambia.

Nash, J. E. & Sutcliffe, J. V., 1970. River flow forecasting through conceptual models: Part 1- A discussion of principals. *Journal of Hydrology,* Issue 10, pp. 282-290.

Nathan, R. J. & McMahon, T. A., 1990. Identification of homogeneous regions for the purpose of regionalisation. *Journal of Hydrology,* Issue 121, pp. 217-238.

Nobrega, M. T., Collischonn, W., Tucci, C. & Paz, A., 2011. Uncertainty in climate change impacts on water resources in the Rio Grande Basin, Brazil. *Hydrology and Earth Sciences,* Issue 15, pp. 585-595.

Oudin, L., Kay, A., Andreassian, V. & Perrin, C., 2010. Are Seemingly physically Similar catchments truly Hydrologically similar?. *Water Resources Research,* Issue 11, p. 46.

Patil, S. & Stieglitz, M., 2012. Controls on Hydrologic similarity: Role of nearby gauged catchments for prediction at an ungauged catchment. *Hydrology and Earth System Sciences,* 2(16), pp. 551-562.

Patil, S. & Stieglitz, M., 2013. Modeling daily streamflow at ungauged catchments: What informationis necessary?. *Hydrological Processes,* Volume 28.

Perrin, C., Michel, C. & Andreassian, V., 2003. Improvement of a parsimonious model for streamflow simulation. *Journal of Hydrology,* pp. 275-289.

Pilgrim, D. H., 1983. Some Problems in transfering hydrological relationships between small and large drainage basins and between regions. *Journal of Hydrology,* Issue 65, pp. 49-72.

Pitchen, G., Mukosa, C. & Cadou, C., 1993. *Recent Hydrological Trends in the Upper Zambezi and Kafue Basins.* Lusaka, International Union for the Conservation of Nature and Natural Resources (IUCN).

Rabus, B., Eineder, M. & A Roth, R. B., 2003. The Shutter radar topography mission (SRTM)- A new class of digital elevation models acquired by spaceborne radar. *Journal of Photogrammetry and Remote Sensing,* 4(57), pp. 241-262.

Randall, B. S., 2006. Introduction to Remote sensing of environment. *Microimages.*
Razavi, T. & Coulibaly, P., 2012. Streamflow prediction in ungauged basins: Review of regionalisation methods. *Hydrology Engineering,* pp. 958-975.

Rosenbrock, H., 1960. An automatic method for finding the greatest or least value of a function. *The Computer Journal,* Volume 3, pp. 175-184.

SADC, 1994. *Wet Season Flow Forecasting for Kariba - Draft Report,* Lusaka: SADC.

SADC, S. A. D. C., 1994. *Hydroelectric Hydrological assistance Project: Compendium of SADC Hydrometric Stations with Telemetry,* Lusaka: SNC Shawinigan.

Santa, J. C., 1978. *Reappraisal of the Power Generation Potential of the Zambezi River at Kariba, Vol.1 CAPCO, HYD-Z-06,* Harare: CAPCO.

Schultz, G. A., 1993. Hydrological Modeling based remote sensing information. *Advanced Space Resource,* 13(5).

Schultz, G. A., 1996. Remote Sensing application in Hydrology. *Hydrological Sciences,* 4(41), pp. 453-475.

Seibert, J., 1997. Estimation of parameter uncertainty in the HBV model. *Nordic Hydrology,* Issue 28, pp. 247-262.

Seibert, J., 2000. Multi-criteria calibration of a conce[tual runoff model using generic algorithm. *Hydrology and earth Sciences,* 2(4), pp. 215-224.

Seth, S., 2008. Role of Remote Sensing and GIS inputs in Physically based hydrolgical medeling.

Sharma, K. D., Soroshian, S. & Wheater, H., 2008. Hydrological Modelling in Arid and Semi-Arid Areas. Issue 5, p. 223.

Shawinigan Engineering, S., 1993. *Water balance Study for Kariba Reservoir- Hydroelectric Hydrological Assistance Project - Phase 2- Draft Report,* Lusaka: SADC AAA.3.4.

Singh, V. P., 1988. *Hydrologic Systems: Rainfall-runoff modelling.* 1 ed. New Jersey: Prentice Hall.

Singh, V. & Woolhiser, D., 2002. Mathematical modelling of Watershed hydrology. *Hydrologic Engineering,* 4(7), pp. 270-292.

Tan, M. L., Latif, A., Pohl, C. & Duan, Z., 2014. Stream flow modelling by remote sensing: A contribution to digital earth. *Earth and Environmental Science,* Issue 18.

Tarboton, D., 1997. A new method for the determination of flow directions and upslope areas in grid digital elevation models. *Water Resources,* 2(33), pp. 309-319.

Tumbare, M. J., 2000. *Management of River Basin and Dams: The Zambezi River Basin.* Ed ed. s.l.:AA Balkema.

Viviroli, D., Mittelbach, H., Gurtz, J. & Weingartner, R., 2009. Continues simulation for flood estimation in ungauged mesoscale catchments of Switzerland-Part 2: Parameter regionalisation and flood estimation results. *Journal of Hydrology,* Issue 377, pp. 208-225.

Vogel, R., 2005. Regional Calibration of watershed models. In: V. Sign & D. Frevert, eds. *Watershed Models.* FL: CRC Press, pp. 549-567.

Wagener, T., Wheater, H. & Gupta, H., 2004. *Rainfall-runoff Modelling in Gauged and Ungauged Catchments.* London: Imperial College Press.

Wang, L. et al., 2010. Developement of an integrated modelling system for improved mulyi-objective reservoir operation. *Frontiers of Architecture and Civil Engineering in China,* 4(1), pp. 47-55.

Wang, Q. et al., 2011. Monthly versus daily water balance in simulating monthly runoff. *Journal of Hydrology,* Issue 404, pp. 166-175.

Winsemius, H., 2009. *Satellite data as complementary information for hydrological modelling: PhD Thesis,* The Netherlands: Delft University of Technology.

Xu, C.-y., 2002. *Hydrologic models.* s.l.:Uppsala University: Department of Earth Sciences: Hydrology.

Yu, S. P. & Yang, T. C., 2000. Using Sythetic flow duration curves for rainfall-runoff model calibration at ungauged sites. *Hydrological process,* 1(14), pp. 117-133.

ZRA, 2005. *Standing Operations Procedures: Kariba Dam and Reservoir,* Lusaka: s.n.

ZRA, Z. R. A., 2010. *Annual Report for the Year Ending 31st December 2010,* Lusaka - zambia: Zambezi River Authority.

APPENDICES

Simulated Hydrographs for the Ungauged Catchments

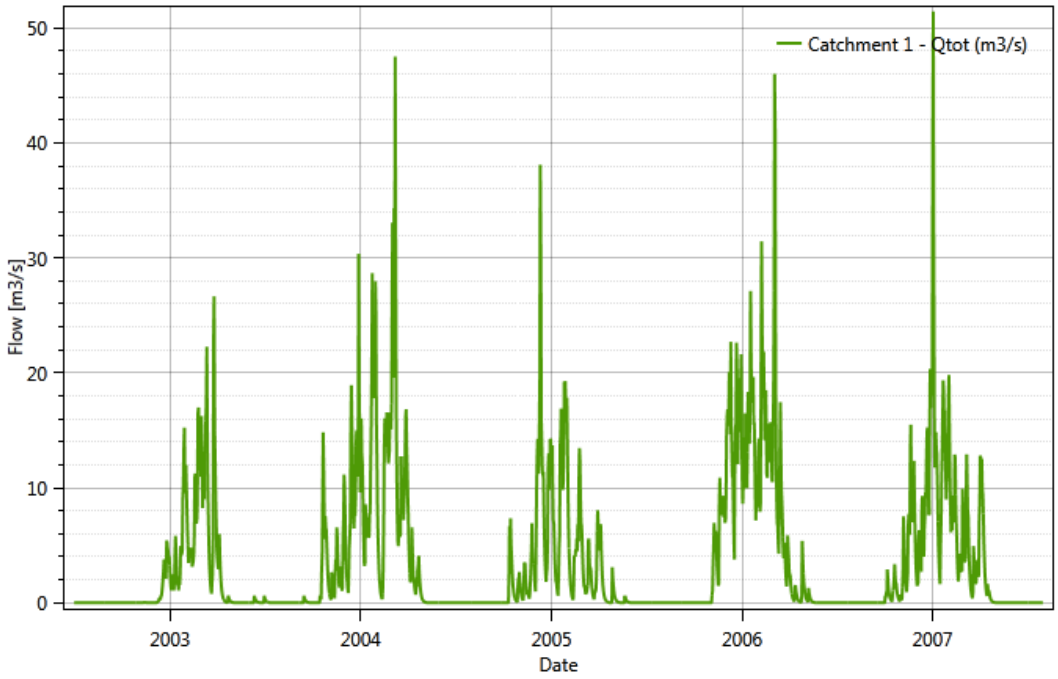

Appendix C_1 Catchment 1 Hydrographs

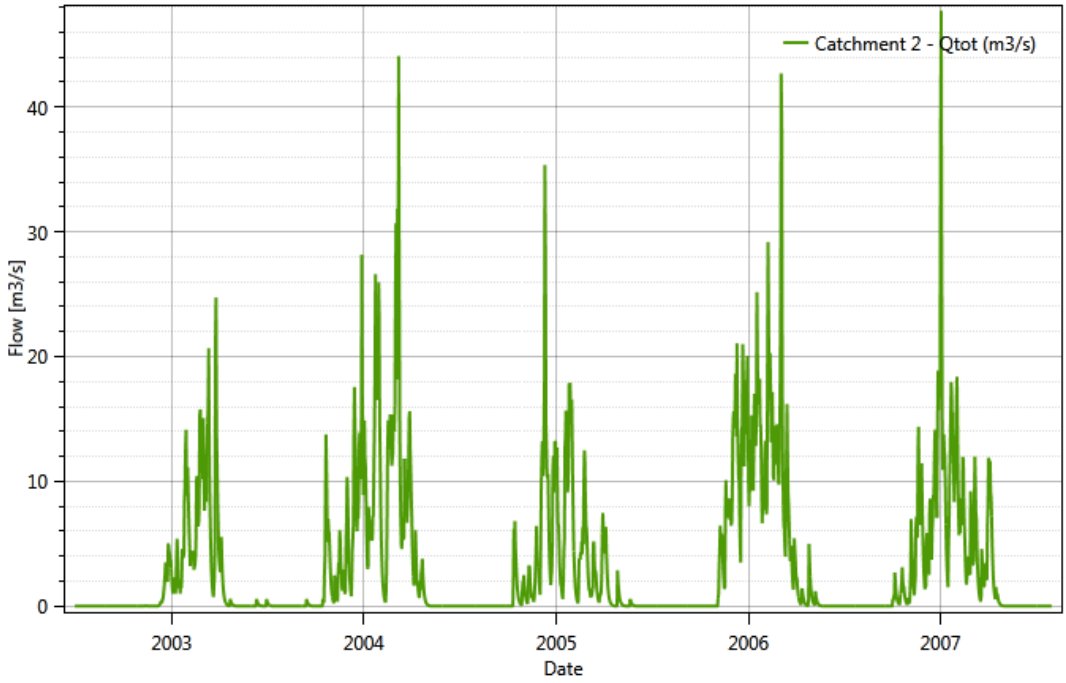

Appendix C_2. Catchment 2 Hydrographs

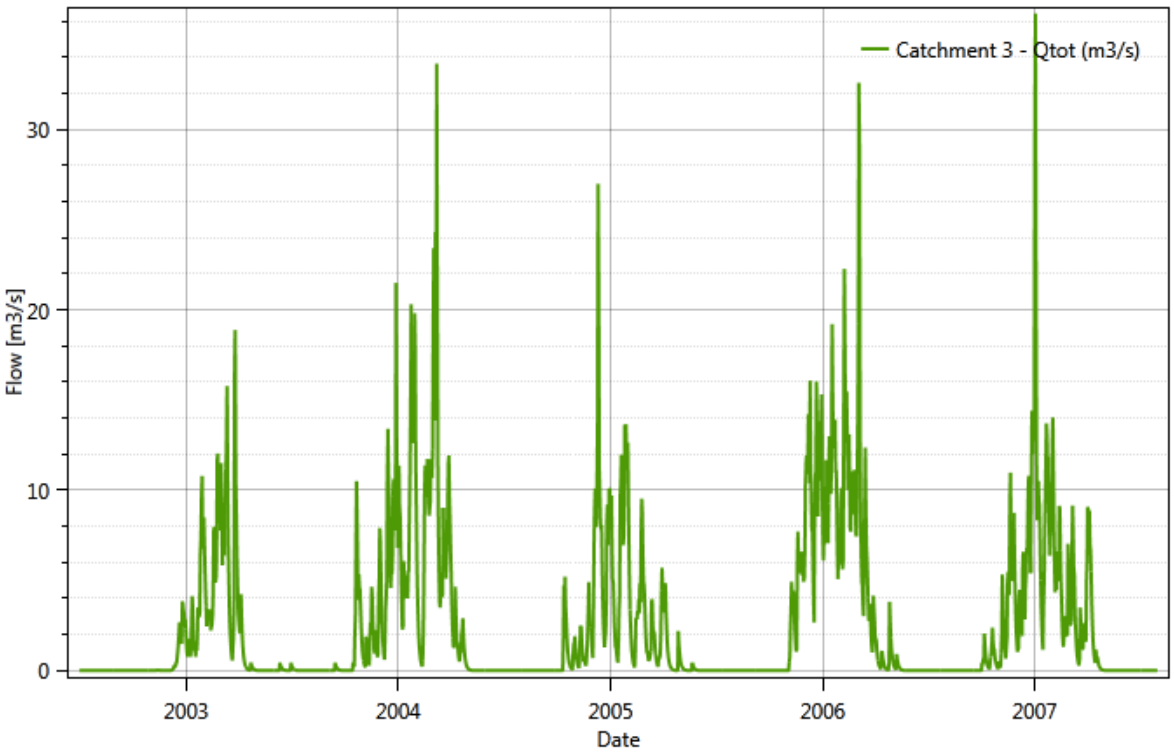

Appendix C_3 Catchment 3 Hydrograph

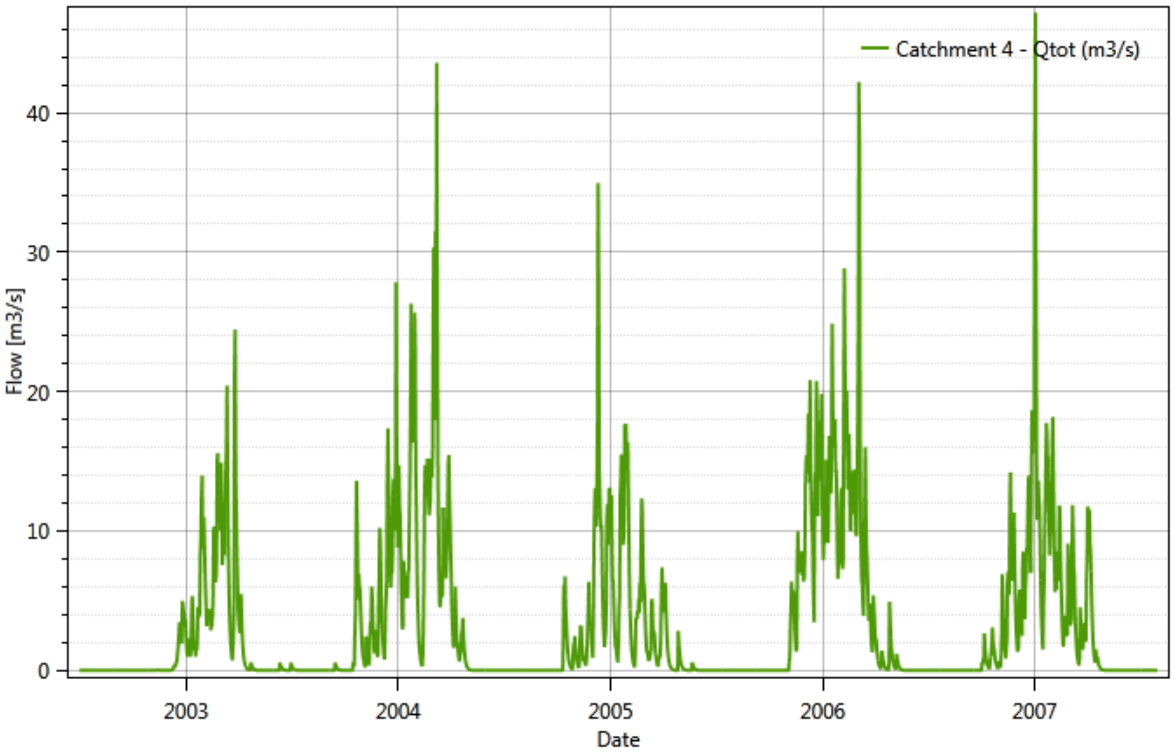

Appendix C_4 Catchment 4 Hydrographs

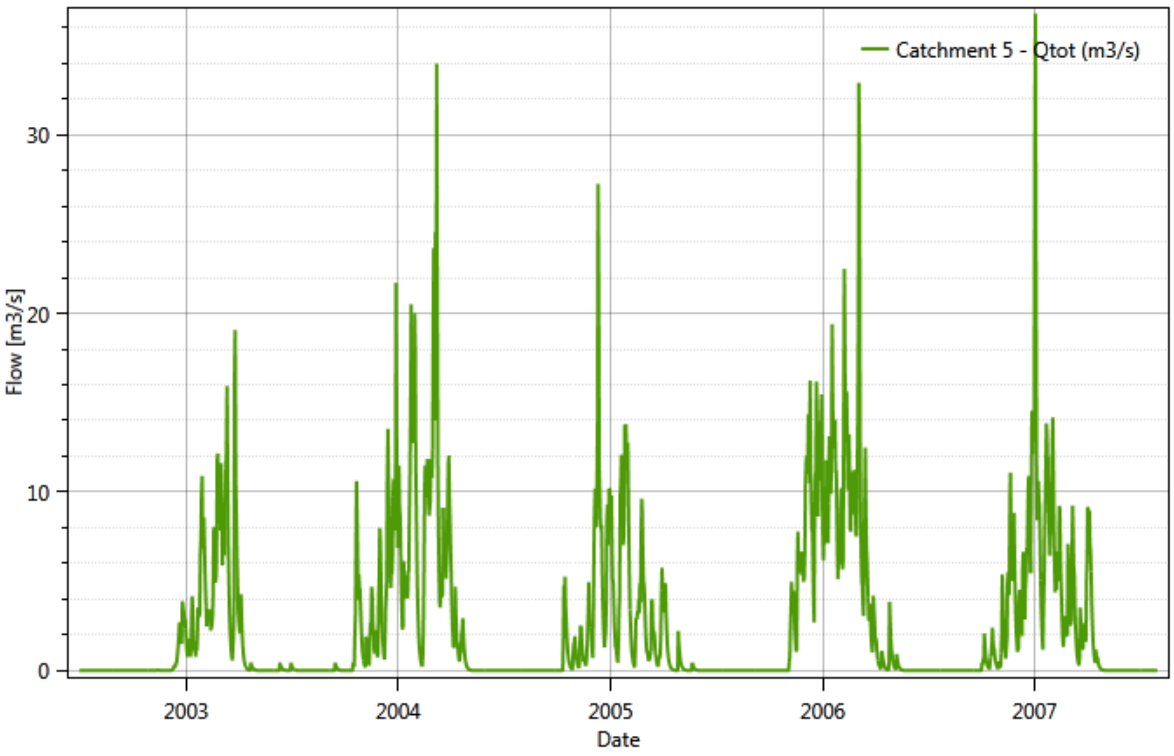

Appendix C_5 Catchment 5 Hydrographs

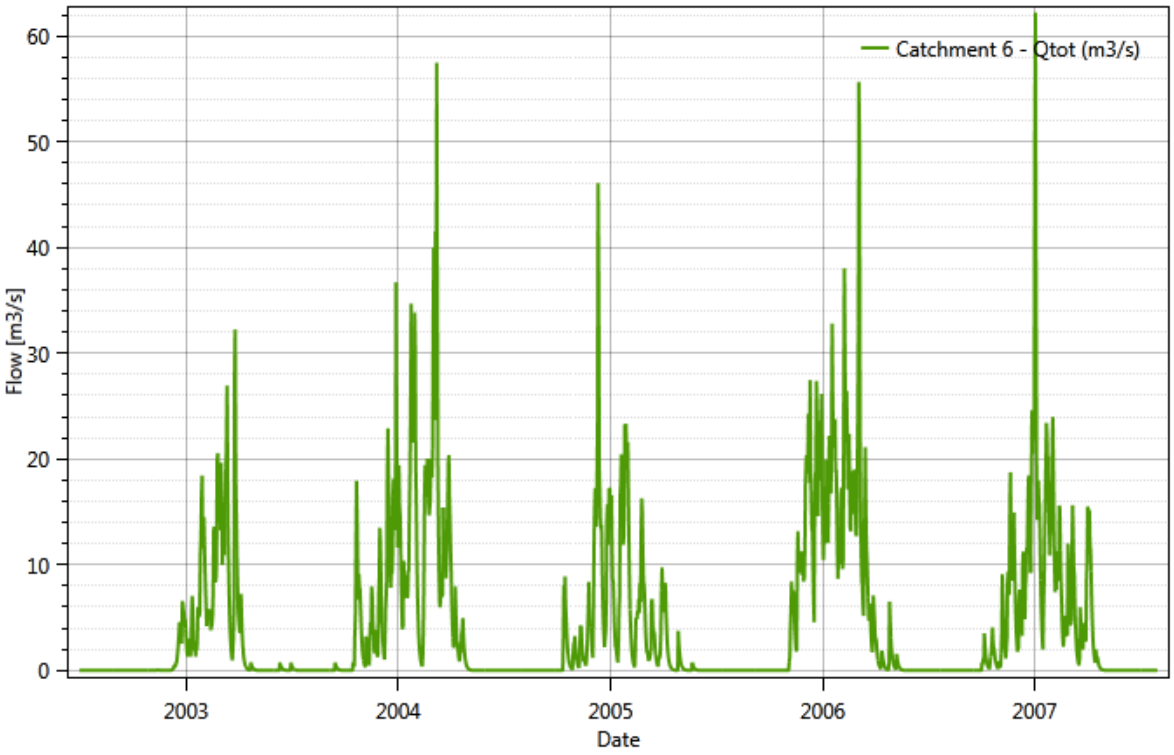

Appendix C_6 Catchment 6 Hydrographs

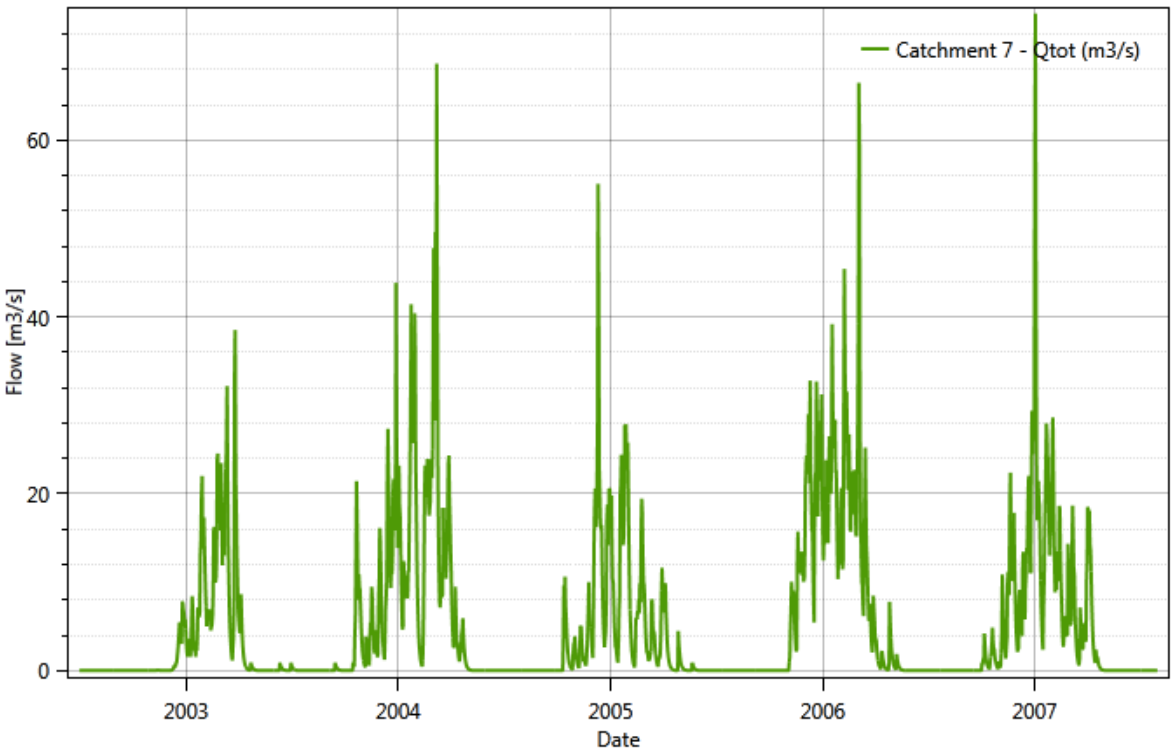

Appendix C_7Catchment 7 Hydrographs

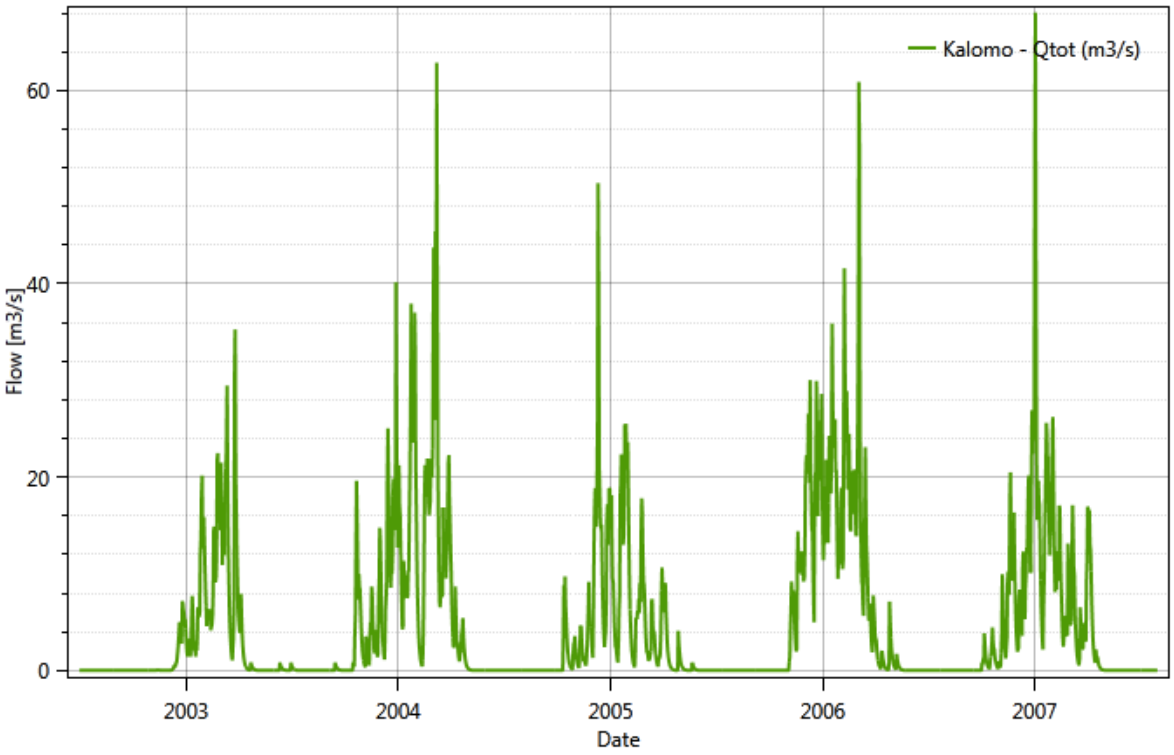

Appendix C_k. Kalomo Catchment Hydrographs

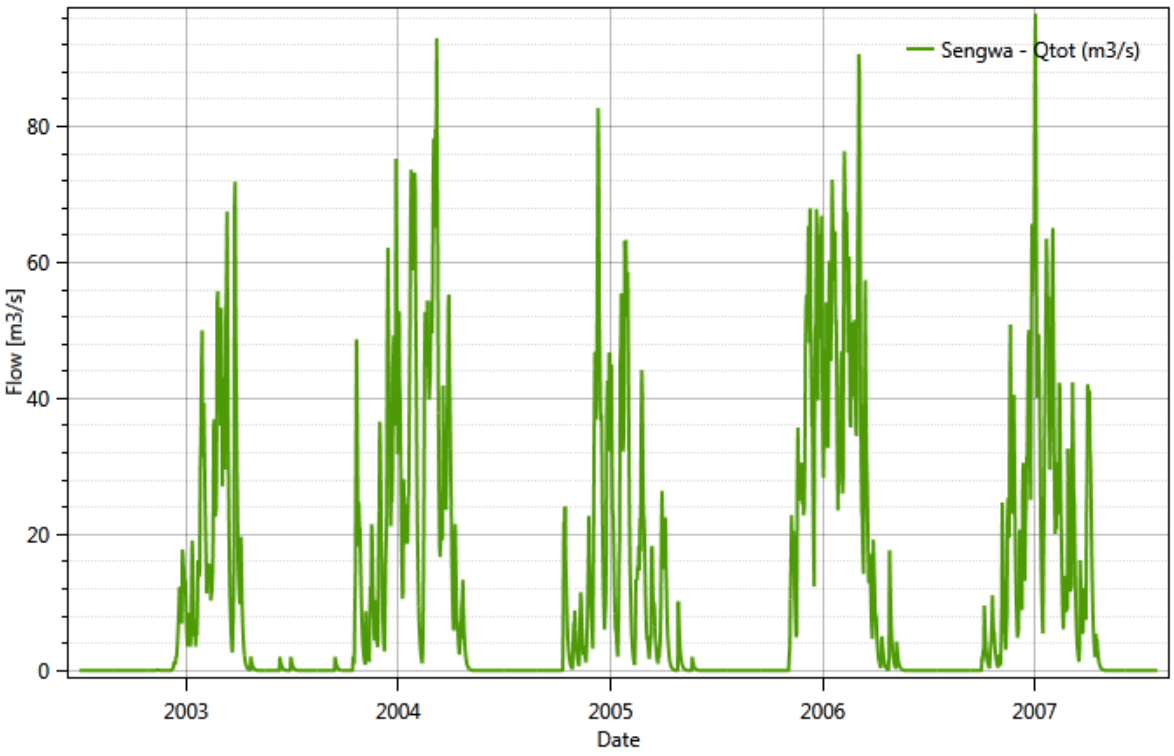

Appendix C_s Sengwa Catchment Hydrographs

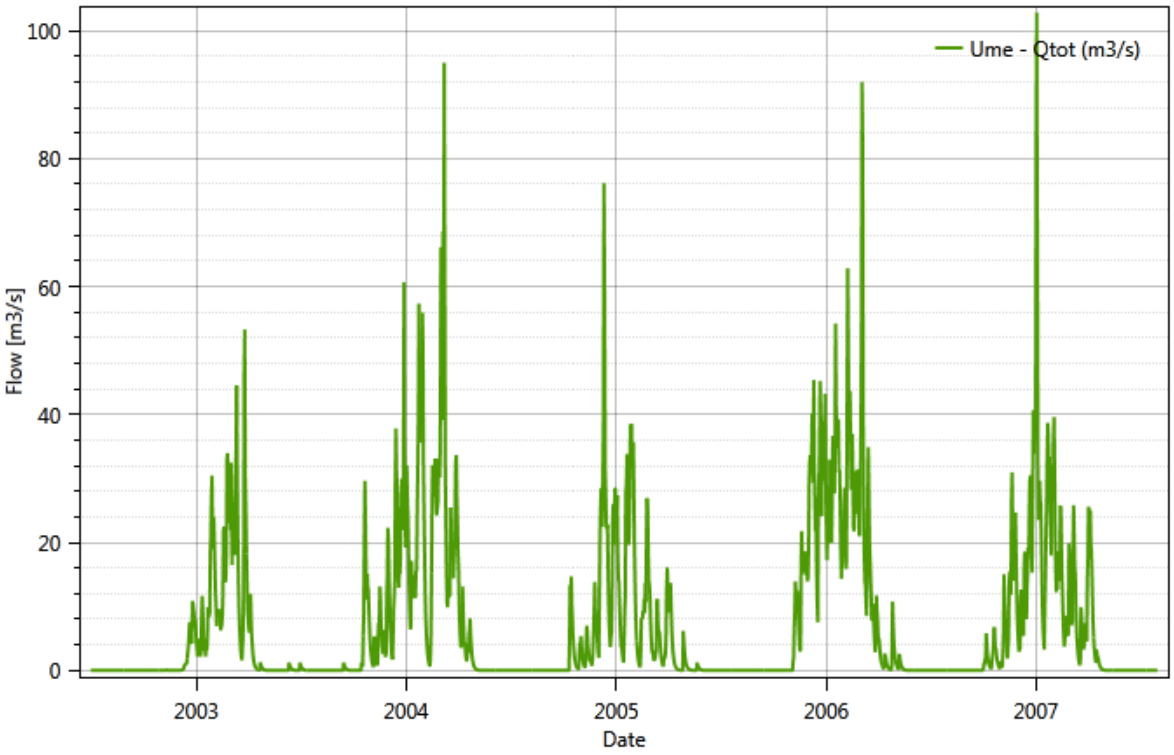

Appendix C_u Ume Catchment Hydrographs